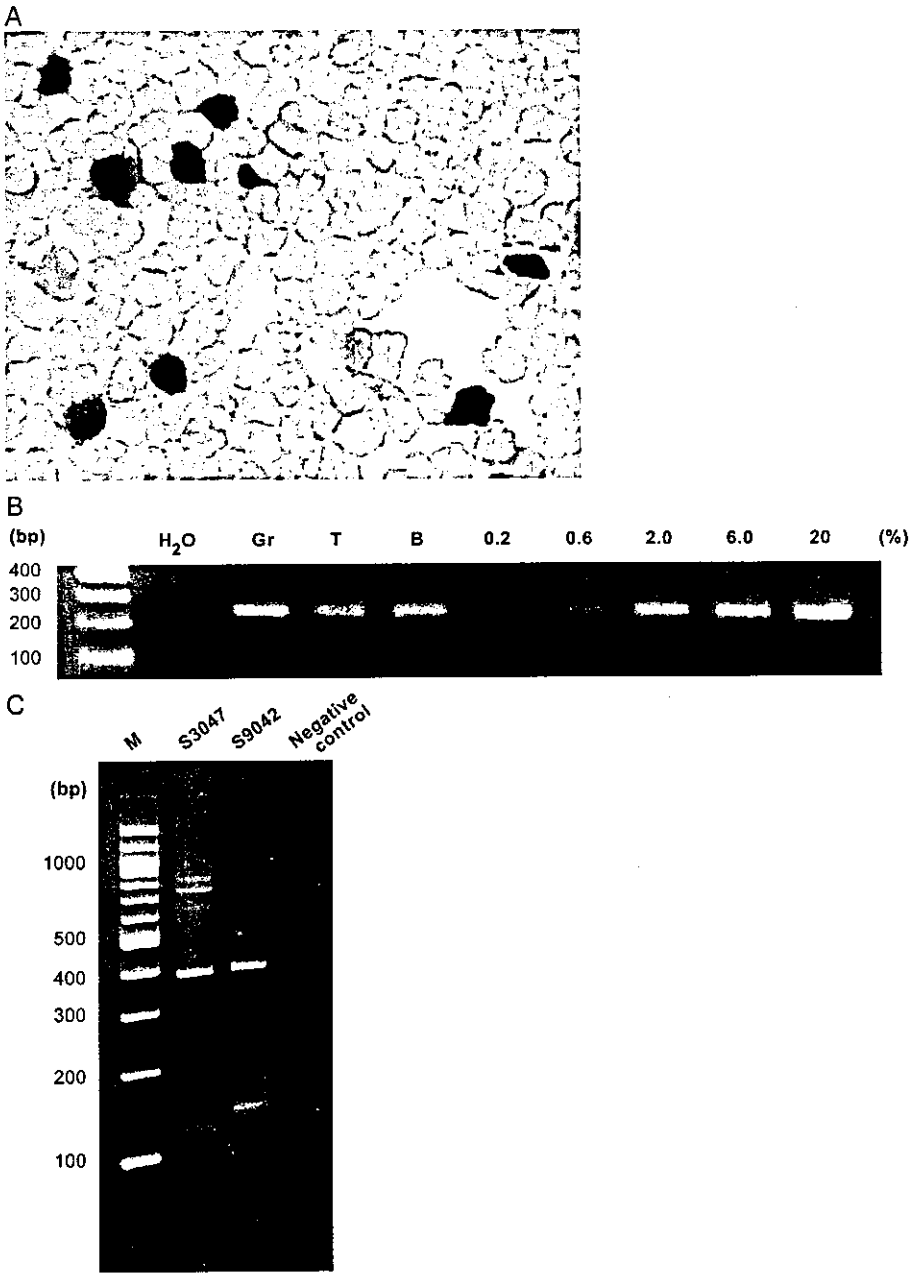

FIG. 4. High-level, multilineage, and polyclonal expansion of gene-modified cells in the peripheral blood after iBMT with SAG in nonconditioned recipients. (A) *In situ* PCR for the provirus. Peripheral blood nucleated cells were collected from animal S9042 receiving EPO at day 89 posttransplantation. Many SAG-transduced cells (stained in black) were detected by *in situ* PCR. (B) Lineage analysis by semiquantitative PCR. DNA from granulocytes (Gr) and T and B lymphocytes sorted from animal S9042 receiving EPO at day 91 posttransplantation was examined for the provirus by semiquantitative PCR. Positive controls corresponding to 0.2, 0.6, 2.0, 6.0, and 20% of transduced cells in peripheral blood were included. (C) Clonal analysis by LAM-PCR. Genomic DNA from peripheral blood of the animals receiving EPO (S9042 at day 90 and S3047 at day 150 posttransplantation) was analyzed by LAM-PCR. Each band indicates different integrants. Negative control was genomic DNA from a naive monkey. M, molecular weight marker.

indicates that the expansion of transduced cells in response to EPO was polyclonal, not mono- or oligoclonal (Fig. 4C).

Dual-Marking Study

We then compared the effects of the SAG vector to a non-SAG vector within, rather than between, individual animals. We harvested cytokine-mobilized peripheral blood $CD34^+$ cells and split them into two equal aliquots. We transduced one aliquot with the SAG vector and the other with the control nonexpression vector (PLI). We mixed both aliquots and returned them by iBMT without marrow conditioning. The animal received EPO from the day after transplantation, and we examined *in vivo* marking levels derived from the two populations by quantitative PCR.

Cells containing the SAG vector increased by 2 logs in the peripheral blood in response to EPO, although cells containing the nonexpression vector remained at low levels (Fig. 5). However, SAG-containing cells were rapidly cleared within 1 month posttransplantation from the periphery and overall SAG-vector marking

doi:10.1016/j.ymthe.2004.06.146

levels became even lower than those from the nonexpression vector-marked fraction. Since cyclosporin A was concomitantly administered to prevent immune responses to human EPO, human EPO concentrations were maintained within an effective range. Thus, it is unlikely that the clearance of xenogeneic human EPO due to immune responses turned off the molecular switch of SAG, resulting in the decrease in SAG-transduced cells.

Immune Responses

The current SAG is a chimeric gene of human origin (the human EPO receptor and human c-Mpl). We collected peripheral lymphocytes from the animal receiving both SAG and nonexpressing PLI (D8058, Fig. 5) at day 169 posttransplantation and examined whether the lymphocytes responded to the xenogeneic SAG *in vitro* (Fig. 6). The response to SAG-transduced target cells was stronger than that to nontransduced target cells (P = 0.05), while the response to PLI-transduced target cells did not differ significantly from that to nontransduced target cells (P = 0.13). The cellular immune response is, therefore, the most likely reason for the clearance of SAG-transduced cells in this animal. This is not novel, but it has been reported that immune responses against transgene products recognized as foreign can indeed be a major obstacle to long-term persistence of gene-modified cells *in vivo* [13,16,17]. In the human clinical setting, however, immune responses should not occur against SAG, because the SAG is made of human genes.

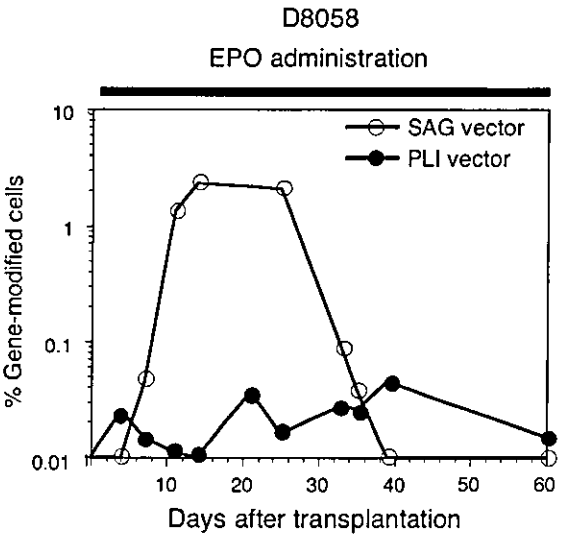

FIG. 5. Dual genetic marking study. CD34$^+$ cells from monkey D8058 were split into two equal aliquots; one aliquot was transduced with SAG vector and the other with nonexpression PLI vector. Both aliquots were together returned to the bone marrow cavity by iBMT without conditioning. EPO (200 IU/kg, twice daily) was administered from the day after transplantation (indicated by a closed bar).

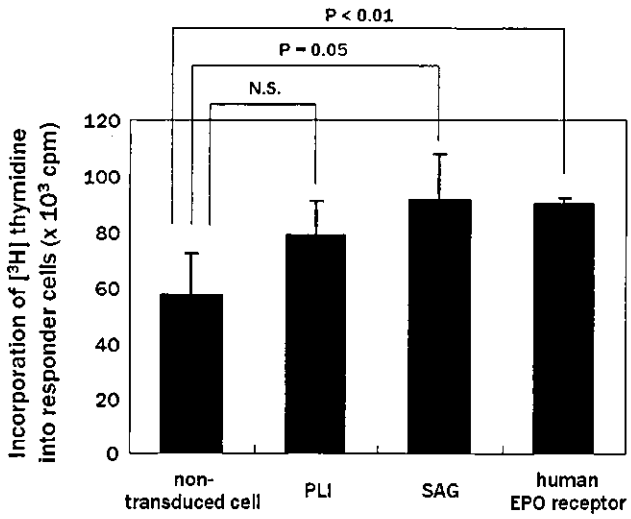

FIG. 6. Positive blastogenic response of lymphocytes to SAG. Peripheral blood mononuclear cells (responder cells) were isolated from monkey D8058 at day 169 posttransplantation (Fig. 5) and cocultured with stimulator cells. The stimulator cells were autologous stromal cells untransduced or transduced retrovirally with PLI, SAG, or human EPO receptor cDNA followed by irradiation with 4000 cGy. After 5 days in culture, the blastogenesis of responder cells was assessed by counting the [^{3}H]thymidine incorporation into responder cells. The averages ± SD of triplicate experiments are shown. N.S., not significant.

Discussion

Previous papers documented that, without marrow conditioning, very low levels (much less than 0.1%) of cells were marked (or corrected) after CD34$^+$ cell gene therapy of chronic granulomatous disease and Gaucher disease [18,19]. This clinical observation has formed the foundation for the contention that myeloablation (or at least conditioning of reduced intensity) is necessary for successful engraftment of transplanted, genetically modified cells. Our results, however, suggest that nonconditioned iBMT results in much higher gene marking levels (up to 8–9%) through the utilization of an SAG. The physical elimination of endogenous marrow with saline before injection might increase gene marking. In the current study, the marrow of four proximal limb bones (femurs and humeri) was replaced with transplanted cells. If other bones such as the iliac bone (which contains more marrow) are similarly used for iBMT, even higher *in vivo* marking levels may be achieved using an SAG.

Expansion of SAG-transduced cells was seen in three lineages: granulocytes, B lymphocytes, and T lymphocytes. The c-Mpl signal generated by the SAG may work even in lymphocytes. In fact, B lymphocytes were shown to be increased by the activated c-Mpl in a canine trans-

plantation model [20]. The expansion was transient, as is the case with other chimeric genes containing c-Mpl as a signal generator [20], although basal marking levels seemed to increase gradually after repeated EPO administration as shown in Fig. 3A. The method largely results in the selection of transduced cells, not at the level of HSCs, but within the differentiated progeny of transduced HSCs.

In the clinical setting, even if the expansion of gene-modified cells is transient, patients can expect therapeutic effects from EPO administration when used as necessary, such as for infection events in patients with chronic granulomatous disease. EPO is a safe drug and can be administered repeatedly with minimal adverse effects. Polycythemia was the only side effect observed in the present study but was manageable by periodic phlebotomy. Therapeutic effects might also be expected from continuously elevated levels of endogenous EPO, such as in patients with thalassemia. When anemia is ameliorated by the gene therapy and endogenous EPO levels return to physiological levels, then the positive selection system is "automatically" turned off, making this a convenient system in such disorders.

Although this "leave it to patients" system would be convenient, a safety concern may be raised regarding leukemogenesis [21]. The SAG proliferation signal that is persistently turned on *in vivo* by endogenous EPO could trigger a secondary event in addition to possible retroviral insertional mutagenesis, although physiological levels of EPO will not induce a significant proliferative response of SAG [12]. Since a set of EPO-mimetic peptides or a modified EPO such as the erythropoiesis stimulating protein has been developed [22,23], it may be possible to develop an SAG containing a mutant EPO receptor that does not bind to endogenous EPO but binds to such EPO-mimetic peptides or modified EPO.

Materials and Methods

Animals. Cynomolgus monkeys (*Macaca fascicularis*) were housed and handled in accordance with the rules for animal care and management of the Tsukuba Primate Center and the guiding principles for animal experiments using nonhuman primates formulated by the Primate Society of Japan. The animals (2.5–5.6 kg, 3–5 years) were certified free of intestinal parasites and seronegative for simian type-D retrovirus, herpesvirus B, varicella-zoster-like virus, and measles virus. The protocol of experimental procedures was approved by the Animal Welfare and Animal Care Committee of the National Institute of Infectious Diseases (Tokyo, Japan).

Collection of cynomolgus CD34⁺ cells. Cynomolgus monkeys received recombinant human (rh) SCF (50 μg/kg; Amgen, Thousand Oaks, CA, USA) and rhG-CSF (50 μg/kg; Chugai, Tokyo, Japan) as daily subcutaneous injections for 5 days prior to blood cell collection. Peripheral blood or bone marrow cells were then collected by leukapheresis or by aspiration from iliac bones, respectively. From the harvested cells, the leukocyte cell fraction was obtained after red blood cell lysis with ACK buffer (155 mM NH_4Cl, 10 mM $KHCO_3$, and 0.1 mM EDTA; Wako, Osaka, Japan). Enrichment of CD34⁺ cells was performed using magnet beads conjugated with anti-human CD34 (clone 561; Dynal, Lake Success, NY, USA), which cross-reacts with cynomolgus CD34 [24]. The purity of CD34⁺ cells ranged from 90 to 95% as assessed with another anti-human CD34 (clone 563; PharMingen, San Diego, CA, USA) which cross-reacts with cynomolgus CD34 [24]. Mean CFU enrichment was 48-fold as assessed by colony-forming progenitor assays performed before and after enrichment.

Retroviral transduction. We used a retroviral vector expressing SAG (a chimeric gene of the human EPO receptor extra- plus transmembrane region and c-Mpl cytoplasmic region) [12] and PLI nonexpression retroviral vector containing untranslated *neo*^{R} and β-*gal* sequences [13]. The titers of the viral supernatants used in the present study were both 1×10^6 particles/ml, as assessed by RNA dot blot. CD34⁺ cells were cultured at a starting concentration of $1–5 \times 10^5$ cells/ml in fresh vector supernatant of PLI or SAG with rhSCF (Amgen), rh thrombopoietin (Kirin, Tokyo, Japan), and rh Flt-3 ligand (Research Diagnostics, Flanders, NJ, USA), each at 100 ng/ml in dishes coated with 20 μg/cm^2 of RetroNectin (Takara, Shiga, Japan). Every 24 h, culture medium was replaced with fresh vector supernatant and cytokines. After 96-h transduction, cells were washed and continued in culture (Dulbecco's modified Eagle's medium (Gibco, Rockville, MD, USA) containing 10% fetal calf serum (Gibco) and 100 ng/ml rhSCF alone) for 2 additional days in the same RetroNectin-coated dishes [25].

Intrabone marrow transplantation. Cynomolgus monkeys were anesthetized. Two needles were inserted into both ends of the femur or humerus [26]. A syringe containing 50 ml of heparin-added saline was connected to one needle and an empty syringe was connected to the other. Normal saline was irrigated gently from one syringe to another through the marrow cavity twice (Fig. 1). Gene-modified cells were suspended in 1 ml of phosphate-buffered saline containing 10% autologous serum and then injected into the marrow cavity and the needle holes were sealed with bone wax (Lukens, Reading, PA, USA). We measured the internal pressure in the marrow cavity during the procedure in some animals and carefully performed saline irrigation and iBMT without inflicting extra pressure on the marrow cavity. No animals suffered from neutropenia, thrombocytopenia, infection, or pulmonary embolism and there was no morbidity. After transplantation, rhEPO (Chugai) was administered to some animals at a dose of 200 IU/kg once or twice daily subcutaneously. Administration of cyclosporin A (Novartis, Basel, Switzerland) to animals was started a week prior to the EPO administration to prevent the development of anti-human EPO antibody [27].

Clonogenic hematopoietic progenitor assays. Cells were plated in a 35-mm petri dish in 1 ml of α-minimum essential medium containing 1.2% methylcellulose (Shin-Etsu Chemicals, Tokyo, Japan) supplemented with 100 ng/ml rh interleukin-3 (PeproTech, Rocky Hill, NJ, USA), 100 ng/ml rh interleukin-11 (PeproTech), 100 ng/ml rhSCF (Biosource, Camarillo, CA, USA), 2 U/ml rhEPO (Roche, Basel, Switzerland), 20% fetal calf serum, 1% bovine serum albumin, 5×10^{-5} M 2-mercaptoethanol (Sigma, St. Louis, MO, USA), and antibiotics (100 U/ml penicillin and 0.1 mg/ml streptomycin). RhEPO was not added to the culture for colony formation from SAG-transduced cells, to avoid excess proliferative response of the transduced cells to EPO. After incubation for 14 days at 37°C with 5% CO_2, colonies containing more than 50 cells were counted using an inverted light microscope. Experiments were conducted in triplicate.

Quantitative PCR. Genomic DNA was extracted using the QIAamp DNA Blood Mini Kit (Qiagen, Chatsworth, CA, USA). DNA (250 ng) was amplified in triplicate with *neo*-specific primers for PLI (5′ -TCCATCATGGATGCAATGCGGC-3′ and 5′ -GATAGAAGGCGATGCGCTGCGAATCG-3′) or with SAG-specific primers (5′ -GACGCTCTCCCTCATCCTCGT-3′ and 5′ -GAGGACTTGGGGAGGATTTCA-3′). Standards consisted of DNA extracted from an SAG- or PLI-producer cell line (which has a known copy number of the proviral sequence) serially diluted with control cynomolgus genomic DNA. Negative controls consisted of DNA extracted from peripheral blood cells of naive monkeys. A β-actin-specific primer set (5′ -

doi:10.1016/j.ymthe.2004.06.146

CCTATCAGAAAGTGGTGGCTGG-3′, 5′-TTGGACAGCAAGAAAGTGAGCTT-3′) was used to certify equal loading of DNA per reaction. Reactions were run using the Qiagen SYBR Green PCR Master Mix (Qiagen) on the ABI Prism 7700 sequence detection system (Applied Biosystems, Foster City, CA, USA) using the following conditions: 50°C for 2 min and 95°C for 15 min, followed by 40 cycles of 94°C for 15 s, 62°C for 30 s, 72°C for 30 s, and 83°C for 15 s. The quantitative PCR was certified each time to yield linear amplifications in the range of the intensity of a positive control series (0.01–100%, correlation coefficient >0.98). For calculating the transduction efficiencies, the C_t value of the vector sequence was normalized based on the C_t value of the internal control β-actin sequence on the same sample as directed in the manufacturer's protocol. Gene marking percentages were calculated given that each provirus-positive cell contains one copy of the vector sequence.

Colony PCR. Well-separated, individual colonies at day 14 were plucked into 50 μl of distilled water, digested with 20 μg/ml proteinase K (Takara) at 55°C for 1 h followed by 99°C for 10 min, and assessed for the SAG or nonexpression PLI vector sequence by nested PCR. The outer primer sets were the same as were used in the quantitative PCR described above. Amplification conditions for the outer PCR were 95°C for 1 min, 54°C for 1 min, and 72°C for 2 min with 20 cycles. The outer PCR products were purified using MicroSpin S-400 HR Columns (Amersham, Piscataway, NJ, USA). The inner primer set for the SAG vector was 5′-CCACCCCTAGCCCTAAATCTTATG-3′ and 5′-GGTGGTTCAGCATCCAATAAGG-3′, and that for the PLI vector was 5′-ATACGCTTGATCCGGCTACCTG-3′ and 5′-GATACCGTAAAGCACGAGGAAG-3′. Amplification conditions for the inner PCR were 95°C for 1 min, 54°C for 1 min, and 72°C for 2 min with 20 cycles. Simultaneous PCR for the β-actin sequence was also performed to certify DNA amplification of the sample in each colony. The primer set for β-actin was the same as was used in the quantitative PCR described above. Amplification conditions for β-actin PCR were 95°C for 1 min, 54°C for 1 min, and 72°C for 2 min with 30 cycles. The final PCR products were separated on 2% agarose gels. The sizes of the products were 206, 483, and 232 bp for SAG, nonexpressing PLI vector, and β-actin sequences, respectively. The transduction efficiency of CFU was calculated by dividing the number of colonies positive for the vector sequence by the number positive for the β-actin sequence. Plucked methylcellulose not containing colonies served as negative controls.

In situ PCR. *In situ* detection of transplanted cell progeny was performed by amplifying the SAG sequence as previously reported [28]. Peripheral blood nucleated cells were spun down to glass slides. The SAG-specific primer sequences were the same as were used for the quantitative PCR described above. The reaction mixture consisted of 420 μM dATP, 420 μM dCTP, 420 μM dGTP, 378 μM dTTP, 42 μM digoxigenin-labeled dUTP (Roche), 0.8 μM each SAG primer, 4.5 mM $MgCl_2$, PCR buffer (Mg^{2+} free), and 4 U Takara *Taq* DNA polymerase (Takara). Slides were covered with the Takara Slide Seal for *in situ* PCR (Takara). PCR was performed using the PTC100 Peltier thermal cycler (MJ Research, Watertown, MA, USA) under the following conditions: 94°C for 1 min and 55°C for 1 min with 15 cycles. The digoxigenin-incorporated DNA fragments were detected using the horseradish peroxidase (HRP)-conjugated rabbit F(ab′) anti-digoxigenin antibody (Dako). Slides were then stained for HRP using the Vector SG Substrate Kit. Finally, slides were counterstained with Kernechtrot dye that stains nucleotides, mounted in glycerol, and examined under a light microscope.

LAM-PCR. The LAM-PCR was performed as previously described [15]. The genomic-proviral junction sequence was preamplified by repeated primer extension using 0.25 pmol of vector-specific, 5′-biotinylated primer LTR1 (5′-AGCTGTTCCATCTGTTCTTGGCCCT-3′) with *Taq* polymerase (2.5 U; Qiagen) from 100 ng of each sample DNA. One hundred cycles of amplification were performed with the addition of fresh *Taq* polymerase (2.5 U) after 50 cycles. Biotinylated extension products were selected with 200 μg of magnetic beads (Dynabeads Kilobase BINDER Kit; Dynal). The samples were incubated with Klenow polymerase (2 U; Roche), dNTPs (300 μM; Pharmacia, Uppsala, Sweden), and a random hexanucleotide mixture (Roche) in a volume of 20 μl for 1 h at 37°C. Samples were washed on the magnetic particle concentrator (Dynal) and incubated with *TasI* (Fermentas, Hanover, MD, USA) to cut the 5′ long terminal repeat-flanking genomic DNA for 1 h at 65°C. After an additional wash step, 100 pmol of a double-stranded asymmetric linker cassette and T4 DNA ligase (6 U; New England Biolabs, Beverly, MA, USA) was incubated with the beads in a volume of 10 μl at 16°C overnight. Denaturing was performed with 5 μl of 0.1 N NaOH for 10 min at room temperature. Each ligation product was amplified with *Taq* polymerase (5 U; Qiagen), 25 pmol of vector-specific primer LTR2a (5′-AACCTTGATCTGAACTTCTC-3′), and linker cassette primer LC1 (5′-GACCCGGGAGATCTGAATTC-3′) by 35 cycles of PCR (denaturation at 95°C for 60 s, annealing at 60°C for 45 s, and extension at 72°C for 60 s). Of each PCR product, 0.2% served as a template for a second, nested PCR with internal primers LTR3 (5′-TCCATGCCTTGCAAAATGGC-3′) and LC2 (5′-GATCTGAATTCAGTGGCACAG-3′) under identical conditions. Final products were separated on a 2% agarose gel.

Flow-cytometric sorting. We used the FSC/SSC profile (forward and side scatter) to sort granulocytes (purity 95%). Anti-CD3 and anti-CD20 were used to sort T lymphocytes (purity 99%) and B lymphocytes (purity 95%), respectively. Cells were sorted using an EPICS Elite cell sorter equipped with an argon-ion laser (Beckman Coulter, Fullerton, CA, USA). Data acquisition and analysis were performed using the EXPO2 software (Beckman Coulter).

Cellular immune response assay. Peripheral blood mononuclear cells and bone marrow stromal cells were isolated from monkey D8058. The stromal cells were transduced with a retroviral vector carrying the PLI, SAG, or human EPO receptor cDNA. The transduced stromal cells were irradiated with 4000 cGy and used as stimulator cells. Untransduced stromal cells irradiated with 4000 cGy served as a control. The peripheral blood mononuclear cells (responder cells, 2×10^5/well) were cocultured with the stimulator or control cells (5×10^4/well) in 96-well, flat-bottom plates with RPMI 1640 medium (Sigma) containing 10% fetal calf serum and 20 IU/ml rh interleukin-2 (Shionogi, Osaka, Japan). After 5 days in culture, the blastogenesis of responder cells was assessed. Briefly, the cells were labeled with 1 μCi/well of [*methyl*-^{3}H]thymidine (Amersham) for 16 h and harvested with an automated cell harvester (Laboratory Science, Tokyo, Japan) onto glass-fiber filters (Molecular Devices, Sunnyvale, CA, USA). The incorporation of [*methyl*-^{3}H]thymidine into responder cells was quantified in a liquid scintillation counter (Aloka, Tokyo, Japan). All experiments were performed in triplicate.

Acknowledgments

We are grateful to Aki Takaiwa and Naomi Terao for technical assistance. We thank Cynthia E. Dunbar for help in performing LAM-PCR. We also thank John F. Tisdale for helpful comments on the manuscript. We acknowledge Novartis' supply of cyclosporin A, Amgen's supply of SCF, Ajinomoto's supply of IL-6, Chugai's supply of G-CSF and EPO, and Kirin's supply of thrombopoietin. This study was supported by the Ministry of Health, Labor, and Welfare of Japan and by the Ministry of Education, Culture, Sports, Science, and Technology of Japan.

RECEIVED FOR PUBLICATION MARCH 1, 2004; ACCEPTED JUNE 7, 2004.

References

1. Cavazzana-Calvo, M., *et al.* (2000). Gene therapy of human severe combined immunodeficiency (SCID)-X1 disease. *Science* **288:** 669–672.
2. Plett, P. A., Frankovitz, S. M., and Orschell-Traycoff, C. M. (2002). In vivo trafficking, cell cycle activity, and engraftment potential of phenotypically defined primitive hematopoietic cells after transplantation into irradiated or nonirradiated recipients. *Blood* **100:** 3545–3552.
3. Bowman, J. E., Reese, J. S., Lingas, K. T., and Gerson, S. L. (2003). Myeloablation is not required to select and maintain expression of the drug-resistance gene, mutant MGMT, in primary and secondary recipients. *Mol. Ther.* **8:** 42–50.

4. Zhong, J. F., Zhan, Y., Anderson, W. F., and Zhao, Y. (2002). Murine hematopoietic stem cell distribution and proliferation in ablated and nonablated bone marrow transplantation. *Blood* **100:** 3521–3526.
5. Nakamura, K., *et al.* (2004). Enhancement of allogeneic hematopoietic stem cell engraftment and prevention of GVHD by intra-bone marrow transplantation plus donor lymphocyte infusion. *Stem Cells* **22:** 125–134.
6. Wang, J., *et al.* (2003). SCID-repopulating cell activity of human cord blood-derived $CD34^-$ cells assured by intra-bone marrow injection. *Blood* **101:** 2924–2931.
7. Mazurier, F., Doedens, M., Gan, O. I., and Dick, J. E. (2003). Rapid myeloerythroid repopulation after intrafemoral transplantation of NOD-SCID mice reveals a new class of human stem cells. *Nat. Med.* **9:** 959–963.
8. Yahata, T., *et al.* (2003). A highly sensitive strategy for SCID-repopulating cell assay by direct injection of primitive human hematopoietic cells into NOD/SCID mice bone marrow. *Blood* **101:** 2905–2913.
9. Ito, K., *et al.* (1997). Development of a novel selective amplifier gene for controllable expansion of transduced hematopoietic cells. *Blood* **90:** 3884–3892.
10. Kume, A., *et al.* (2003). In vivo expansion of transduced murine hematopoietic cells with a selective amplifier gene. *J. Gene Med.* **5:** 175–181.
11. Hanazono, Y., *et al.* (2002). In vivo selective expansion of gene-modified hematopoietic cells in a nonhuman primate model. *Gene Ther.* **9:** 1055–1064.
12. Nagashima, T., *et al.* (2004). In vivo expansion of gene-modified cells by a novel selective amplifier gene utilizing the erythropoietin receptor as a molecular switch. *J. Gene Med.* **6:** 22–31.
13. Heim, D. A., *et al.* (2000). Introduction of a xenogeneic gene via hematopoietic stem cells leads to specific tolerance in a rhesus monkey model. *Mol. Ther.* **1:** 533–544.
14. Horsfall, M. J., Hui, C. H., To, L. B., Begley, C. G., Basser, R. L., and Simmons, P. J. (2000). Combination of stem cell factor and granulocyte colony-stimulating factor mobilizes the highest number of primitive haemopoietic progenitors as shown by pre-colony-forming unit (pre-CFU) assay. *Br. J. Haematol.* **109:** 751–758.
15. Schmidt, M., *et al.* (2003). Clonality analysis after retroviral-mediated gene transfer to $CD34^+$ cells from the cord blood of ADA-deficient SCID neonates. *Nat. Med.* **9:** 463–468.
16. Riddell, S. R., *et al.* (1996). T-cell mediated rejection of gene-modified HIV-specific cytotoxic T lymphocytes in HIV-infected patients. *Nat. Med.* **2:** 216–223.
17. Rosenzweig, M., *et al.* (2001). Induction of cytotoxic T lymphocyte and antibody responses to enhanced green fluorescent protein following transplantation of transduced CD34(+) hematopoietic cells. *Blood* **97:** 1951–1959.
18. Malech, H. L., *et al.* (1997). Prolonged production of NADPH oxidase-corrected granulocytes after gene therapy of chronic granulomatous disease. *Proc. Natl. Acad. Sci. USA* **94:** 12133–12138.
19. Dunbar, C. E., *et al.* (1998). Retroviral transfer of the glucocerebrosidase gene into CD34+ cells from patients with Gaucher disease: in vivo detection of transduced cells without myeloablation. *Hum. Gene Ther.* **9:** 2629–2640.
20. Neff, T., *et al.* (2002). Pharmacologically regulated in vivo selection in a large animal. *Blood* **100:** 2026–2031.
21. Hacein-Bey-Abina, S., *et al.* (2003). LMO2-associated clonal T cell proliferation in two patients after gene therapy for SCID-X1. *Science* **302:** 415–419.
22. Wrighton, N. C., *et al.* (1996). Small peptides as potent mimetics of the protein hormone erythropoietin. *Science* **273:** 458–464.
23. Macdougall, I. C. (2000). Novel erythropoiesis stimulating protein. *Semin. Nephrol.* **20:** 375–381.
24. Shibata, H., *et al.* (2003). Collection and analysis of hematopoietic progenitor cells from cynomolgus macaques (Macaca fascicularis): assessment of cross-reacting monoclonal antibodies. *Am. J. Primatol.* **61:** 3–12.
25. Takatoku, M., *et al.* (2001). Avoidance of stimulation improves engraftment of cultured and retrovirally transduced hematopoietic cells in primates. *J. Clin. Invest.* **108:** 447–455.
26. Kushida, T., *et al.* (2002). Comparison of bone marrow cells harvested from various bones of cynomolgus monkeys at various ages by perfusion or aspiration methods: a preclinical study for human BMT. *Stem Cells* **20:** 155–162.
27. Schuurman, H. J., *et al.* (2001). Pharmacokinetics of cyclosporine in monkeys after oral and intramuscular administration: relation to efficacy in kidney allografting. *Transplant. Int.* **14:** 320–328.
28. Haase, A. T., Retzel, E. F., and Staskus, K. A. (1990). Amplifications and detection of lentiviral DNA inside cells. *Proc. Natl. Acad. Sci. USA* **87:** 4971–4975.

ELSEVIER

EXPERIMENTAL HEMATOLOGY

Experimental Hematology 32 (2004) 375–381

Ascorbic acid restores sensitivity to imatinib via suppression of Nrf2-dependent gene expression in the imatinib-resistant cell line

Takahisa Tarumoto[a], Tadashi Nagai[a], Ken Ohmine[a], Takuji Miyoshi[a], Makiko Nakamura[a], Takahito Kondo[b], Kenji Mitsugi[c], Syuji Nakano[c], Kazuo Muroi[d], Norio Komatsu[a], and Keiya Ozawa[a]

Divisions of [a]Hematology and [d]Cell Transplantation and Transfusion, Jichi Medical School, Tochigi, Japan; [b]Department of Biochemistry and molecular Biology in Disease, Atomic Bomb Disease Institute, Nagasaki University Graduate School of Medicine, Nagasaki, Japan; [c]First Department of Internal Medicine, Faculty of Medicine, Kyushu University, Fukuoka, Japan

(Received 11 August 2003; revised 1 December 2003; accepted 15 January 2004)

Objective. **Imatinib, a BCR/ABL tyrosine kinase inhibitor, has shown remarkable clinical effects in chronic myelogenous leukemia. However, the leukemia cells become resistant to this drug in most blast crisis cases. The transcription factor Nrf2 regulates the gene expression of a number of detoxifying enzymes such as γ-glutamylcysteine synthetase (γ-GCS), the rate-limiting enzyme in glutathione (GSH) synthesis, via the antioxidant response element (ARE). In this study, we examined the involvement of Nrf2 in the acquisition of resistance to imatinib. Since oxidative stress promotes the translocation of Nrf2 from the cytoplasm to the nucleus, we also examined whether ascorbic acid, a reducing reagent, can overcome the resistance to imatinib by inhibiting Nrf2 activity.**

Results. **Binding of Nrf2 to the ARE of the γ-GCS light subunit (γ-GCSl) gene promoter was much stronger in the imatinib-resistant cell line KCL22/SR than in the parental imatinib-sensitive cell line KCL22. The levels of γ-GCSl mRNA and GSH were higher in KCL22/SR cells, a finding consistent with the observation of an increase in Nrf2-DNA binding. Addition of a GSH monoester to KCL22 cells resulted in an increase in the IC_{50} value of imatinib. In contrast, addition of ascorbic acid to KCL22/SR cells resulted in a decrease in Nrf2-DNA binding and decreases in levels of γ-GCSl mRNA and GSH. Consistent with these findings, ascorbic acid partly restored imatinib sensitivity to KCL22/SR.**

Conclusion. **Changes in the redox state caused by antioxidants such as ascorbic acid can overcome resistance to imatinib via inhibition of Nrf2-mediated gene expression.** © **2004 International Society for Experimental Hematology. Published by Elsevier Inc.**

Imatinib (imatinib mesylate: Novartis Pharmaceuticals, Basel, Switzerland), a specific BCR/ABL tyrosine kinase inhibitor, has been shown to be effective for treatment of chronic myelogenous leukemia (CML) in blast crisis (BC) and in chronic phase (CP) [1–2]. In recent clinical studies of imatinib with large numbers of BC patients, around 50% of patients achieved hematologic response [3]. However, drug resistance is a major problem for imatinib treatment of CML patients in BC because substantial numbers of patients have relapsed relatively soon after treatment with imatinib [2,3]. Previous studies have demonstrated possible mechanisms involved in resistance to imatinib. These include amplification of and mutations in the BCR/ABL gene, increased expression of BCR/ABL protein and p-glycoprotein, and an increase in serum α1 acid glycoprotein [4–9]. However, some imatinib-resistant cells show none of these changes [6], suggesting that the mechanisms involved in resistance to imatinib are very complex.

Nrf2, a member of the CNC family of basic region-leucine zipper transcription factors, has been shown to bind to antioxidant-responsive element (ARE) [10,11]. ARE has been found in the promoter region of several detoxifying and antioxidative stress genes such as γ-glutamylcystein synthetase (γ-GCS) and glutathione-S-transferase (GST). Nrf2 contains 6 conserved domains: Neh1 to Neh6. Previous analysis has shown that Keap1, a homologue of the Drosophila actin-binding protein Kelch, binds to the Neh2 domain of Nrf2

Offprint requests to: Tadashi Nagai, M.D., Ph.D., Jichi Medical School, 3311-1 Yakushiji, Minamikawachi-machi, Kawachi-gun, Tochigi 329-0498, Japan; E-mail: t-nagai@jichi.ac.jp

0301-472X/04 $–see front matter.
doi: 10.1016/j.exphem.2004.01.007

in cytoplasm in a "nonstimulated"condition [12]. Activation inducers for Nrf2 such as oxidative stress cause dissociation of these two factors, resulting in migration of Nrf2 into the nucleus. There, Nrf2 binds to ARE as a heterodimer with other transcription factors, such as small Maf family proteins, and regulates ARE-mediated gene expression. Because induction of phase II detoxifying enzymes is significantly reduced in Nrf2 knockout mice and induction of some antioxidative stress genes such as hemeoxygenase I is severely impaired in Nrf2-deficient macrophages [13,14], it is thought that Nrf2 is necessary for expression of antioxidative stress genes as well as phase II detoxifying enzymes.

γ-GCS, the rate-limiting enzyme of the glutathione (GSH) synthetic pathway, catalyzes condensation of L-glutamate and L-cystein, to form L-γ-glutamylcysteine [15]. GSH, a prominent cellular nonprotein thiol, functions as a cellular antioxidant, and is thus critical for maintenance of redox balance [16]. In addition to these functions, it has been shown that GSH has effects on MAP kinase signaling and activity of the transcription factor NF-κB [17–19]. Also, it is involved in detoxification of substances in cells, via conjugation and transportation of substances out of cells [20]. Previous studies show that GSH is involved in resistance to some anti-cancer drugs, including cisplatin, doxorubicin, cytosine arabinoside, and daunorubicin [21,22]. γ-GCS is a heterodimer of heavy and light subunits: the catalytic domain is in the heavy subunit; the light subunit is important for regulation of the enzyme activity. Analysis of structure and function of the γ-GCS gene has shown that several cis-elements, including AP-1 and NF-κB binding sites, may be important in expression of this gene, and indicates that ARE is critical for expression of this gene [23].

In the present study, we found that γ-GCSl mRNA levels, GSH concentration, and levels of Nrf2/DNA complex at the ARE of the γ-GCS light subunit (γ-GCSl) gene promoter were higher in the imatinib-resistant BCR/ABL$^+$ cell line KCL22/SR than in the imatinib-sensitive parental cell line KCL22. We also found that ascorbic acid (AA) suppressed migration of Nrf2 to the nucleus, resulting in inhibition of GSH synthesis and restoration of sensitivity to imatinib in KCL22/SR cells.

Materials and methods

Cell culture

KCL22 is a BCR/ABL$^+$ cell line that was established from peripheral blood cells of a patient with CML in BC [24]. KCL22/SR is an imatinib-resistant cell line that was derived from KCL22 in our laboratory [25]. Cells from these lines were grown in RPMI1640 medium supplemented with 10% fetal bovine serum and split every 3 to 4 days. KCL22/SR cells were maintained in the presence of 0.5 mM imatinib. To evaluate effects of GSH on sensitivity of KCL22 cells to imatinib, KCL22 cells were incubated in the presence of 10 mM glutathione monoestel [26] for 24 hours prior to addition of various concentrations of imatinib. An MTT [3-(4,5-dimethylthiazol-2-yl)-2,5-diphenyl tetrazolium bromide] assay was performed to evaluate cytotoxicity, and IC_{50} values were determined from dose-response curves. To examine effects of AA, KCL22/SR cells were cultured without imatinib for 3 days, and were then incubated with 0.5 mM imatinib or 0.125 mM AA for 72 hours. Viable cells were counted by trypan blue exclusion after various periods of incubation.

Determination of glutathione concentration

A total of 2×10^6 cells were harvested and used to assay for glutathione. Glutathione concentration was measured using the GSH-400 system (OXIS Int. Inc., Portland, OR, USA), essentially according to the manufacturer's protocol.

Determination of intracellular peroxides in KCL22/SR cells

Cells were incubated with 2′,7′-dichlorofluorescein diacetate (Molecular Probes, Eugene, OR, USA) as the fluorogenic substrate for 30 minutes. The level of intracellular peroxides was determined by flow cytometry, as described previously [27].

RNA blot analysis

Total RNA was isolated from KCL22 and KCL22/SR cells using the acid guanidium thiocyanate–phenol chloroform method [28]. Northern blot analysis was performed as described elsewhere [29]. Human cDNA clones of γ-GCS light and heavy subunits [21] were used as probes. The HG126 clone of the ribosomal RNA gene was used as an internal control.

Western blot analysis

Total cell lysate and nuclear extract were prepared from 1×10^7 cells, using a method described elsewhere [30]. Protein concentration was determined using a Protein Assay Kit (BioRad, Hercules, CA, USA). A 10% polyacrylamide gel was used to separate 10 μg of protein electrophoretically. Immunoblotting and detection by enhanced chemiluminescence were performed as described elsewhere [31]. Rabbit polyclonal anti-Nrf2 (C-20) antibody was purchased from Santa Cruz Biotechnology, Inc. (Santa Cruz, CA, USA). Mouse anti-glyceraldehyde-3-phosphate dehydrogenase monoclonal antibody, which was used as an internal control, was purchased from Chemicon International (Temecula, CA, USA).

DNA gel mobility shift assays

To evaluate the DNA binding activity of Nrf2, DNA gel mobility shift assays were performed using the oligomer 5′-CTACGATTTC-TGCTTAGTCATTGTCTTCC-3′, which contains the 11-bp ARE and its flanking sequences. This oligomer was end-labeled with [γ-^{32}P] ATP by T4 polynucleotide kinase (Boehringer Mannheim Corp., Indianapolis, IN, USA). The antisense oligomer was then added to the ^{32}P-end-labeled oligomer to yield a double-stranded probe. Nuclear extracts (5 μg) were incubated with the ^{32}P-labeled oligomer for 15 minutes on ice, in a reaction mixture containing 20 mM HEPES buffer (pH 7.8), 60 mM KCl, 0.2 mM EDTA, 6 mM $MgCl_2$, 0.5 mM dithiothreitol (DTT), 10% [v/v] glycerol and 1.5 μg of an equimolar mixture of poly (dI-dC) and poly (dA-dT). For competition assays, the AREm oligomer 5′-CTACGATTTCTGCTTCGTCCTTGTCTTCC-3′, which is a mutated ARE containing two transversions, was used in double-stranded form. In antibody-mediated competition assays, 3 μL of anti-Nrf1, anti-Nrf2, anti-c-Jun, and anti-GATA-2 antibodies (Santa Cruz Biotechnology, Inc., Santa Cruz, CA, USA) were first incubated with nuclear extracts on ice for 20 minutes and were then incubated with the probes for 10 minutes. This mixture was then

loaded onto a 4% polyacrylamide gel and electrophoresed at 150 V and 4°C.

Transfection and luciferase assays

We cotransfected 2 μg of luciferase reporter plasmid fused to human γ-GCSl promoter region (pGCSl-pro; contains ARE and AP-1 binding sites) and 1 μg of effector plasmid or pRL-CMV (internal control) into KCL22/SR cells using TransFast reagent (Promega Corp., Madison, WI, USA), according to the manufacturer's protocol. Briefly, a total of 1×10^6 cells were incubated with the plasmids and TransFast, in 1 mL of medium without serum for 1 hour. Then, 5 mL of fresh medium containing 10% serum was added, and incubation was continued for 48 hours. Luciferase activity was determined using the Dual-Luciferase Reporter Assay System (Promega). Effector plasmids expressing full-length (pcDNA3/mNrf2#0) and dominant-negative (pcDNA3/mNrf2#Eco del) mouse Nrf2 were kindly provided by Drs. K. Ito and M. Yamamoto (Tsukuba University, Tsukuba, Japan).

Results

Formation of Nrf2/DNA complex at ARE was increased in KCL22/SR cells

It has been reported that ARE binds with CNC family transcription factors and plays a critical role in expression of a number of antioxidant and detoxifying enzymes such as γ-GCS, which is a rate-limiting enzyme in GSH synthesis. To clarify whether ARE-mediated regulation of gene expression is involved in imatinib resistance, we first examined DNA binding activity at ARE in the human γ-GCSl gene promoter of KCL22 and KCL22/SR cells using a gel mobility shift assay. The band that was detected was much more prominent in KCL22/SR than in KCL22 (Fig. 1A). This band was completely suppressed by addition of anti-Nrf2 antibody, but not by anti-Nrf1, anti-c-Jun, or anti-GATA-2 antibodies, indicating that it is an Nrf2/DNA complex (Fig. 1B). The increase in Nrf2/DNA complex formation in KCL22/SR cells is not due to increased Nrf2 expression, because there was no difference in Nrf2 protein level between KCL22 and KCL22/SR cells when total cell lysate was used for immunoblot analysis (Fig. 1C). However, when nuclear extracts were used for immunoblot analysis, the level of Nrf2 protein was much higher in KCL22/SR cells than in KCL22 cells (Fig. 1C). These results suggest that induction of Nrf2/DNA complex formation in KCL22/SR cells is caused by movement of Nrf2 from cytoplasm to nucleus.

Nrf2 increased γ-GCS light subunit gene promoter activity

To clarify whether the Nrf2/DNA complex is active in transcription, we examined the effect of Nrf2 on ARE-mediated promoter activation by luciferase reporter assay. Results of these experiments are summarized in Figure 2. When pGCS-pro, which contains ARE and AP-1 sites, was transfected into KCL22/SR cells, luciferase activity increased 150-fold over control activity, which was obtained by transfection of pGL3-Basic promoterless construct. Cotransfection of

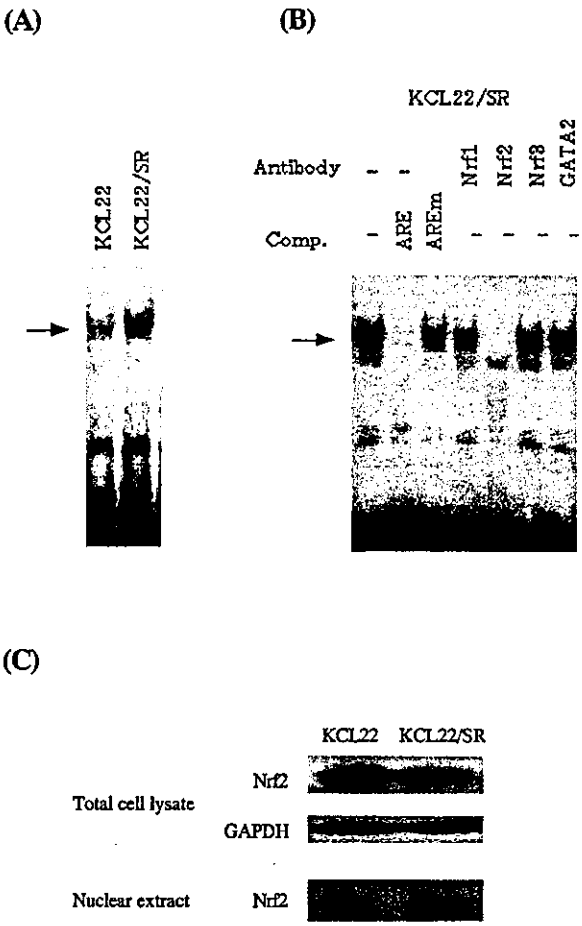

Figure 1. Formation of a DNA-protein complex at antioxidant responsive element (ARE) of the human γ-glutamylcystein synthetase light subunit (γ-GCSl) gene promoter. (A): Nuclear extracts (5-mg aliquots) from KCL22 or KCL22/SR cells were incubated with end-labeled oligomers corresponding to ARE. (B): Competition assays were performed with a 200-fold molar excess of the indicated oligonucleotides or anti-Nrf2, anti-Nrf1, anti-c-Jun, and anti-GATA-2 antibodies. (C): Total cell extracts or nuclear extracts were prepared, separated by SDS-polyacrylamide gel electrophoresis, transferred onto a membrane, and reacted with anti-Nrf2 antibody. The expression of glyceraldehyde-3-phosphate dehydrogenase (GAPDH) was examined as an internal control.

the Nrf2 expression vector pcDNA3/Nrf2#0 resulted in a significant increase in luciferase activity. In contrast, expression of the dominant-negative form of Nrf2, which lacks the transcriptional activation domain (pcDNA3/mNrf2#Eco del), suppressed luciferase activity (Fig. 2). These results suggest that ARE in the γ-GCSl gene promoter is active in transcription, and that induction of Nrf2/DNA complex formation at ARE leads to upregulation of promoter activity.

GSH level is higher in KCL22/SR than in KCL22 cells

The level of γ-GCSl mRNA was significantly higher in KCL22/SR cells than in KCL22 cells (Fig. 3A), and the concentration of GSH was 1.5-fold higher in KCL22/SR cells than in KCL22 cells (Fig. 3B). Because γ-GCS is a rate-limiting enzyme of GSH synthesis, upregulation of γ-GCSl

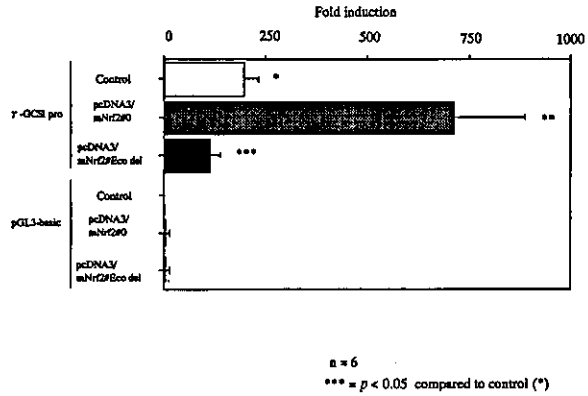

Figure 2. Effect of Nrf2 on the enhancer activity of the human γ-GCSl gene promoter. KCL22/SR cells were transfected with luciferase reporter pGCS-pro or pGL3-Basic together with 1 μg each of pcDNAmNrf2#0 or pcDNA3mNrf2#Eco del effector molecules. Firefly luciferase activity was normalized on the basis of Renilla luciferase activity. The results are expressed as the ratio of firefly luciferase activities of cells transfected with pGL3-basic without any effector molecule.

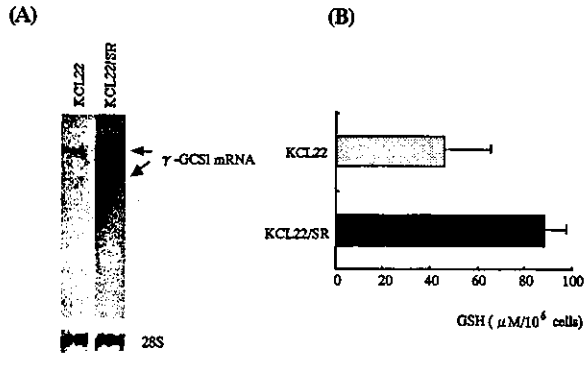

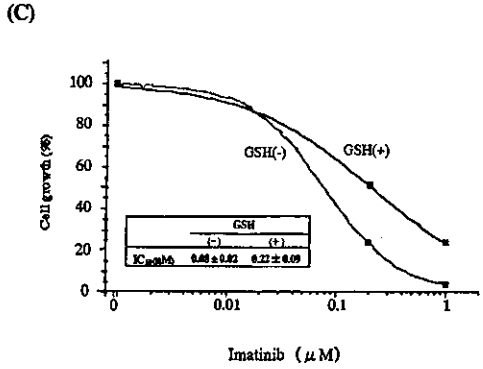

Figure 3. Glutathione synthesis in KCL22/SR cells. **(A)**: The levels of γ-GCSl mRNA were analyzed by Northern blotting. The filter was rehybridized to a ribosomal RNA probe. 28S ribosomal RNA bands are shown. **(B)**: Glutathione (GSH) concentration was measured with the GSH-400 system (OXIS Int. Inc.), using 2×10^6 KCL22 or KCL22/SR cells, as described in Materials and Methods. **(C)**: KCL22 cells were cultured with various concentrations of imatinib for 72 hours in the presence or absence of GSH. The ratio of IC_{50} is shown in the figure.

expression may lead to accumulation of GSH in KCL22/SR cells.

In previous studies, GSH was implicated in resistance to some anti-cancer drugs [9,10]. To clarify whether increased GSH levels are important for resistance to imatinib, we examined the effect of a GSH monoester on sensitivity to imatinib. Addition of a GSH monoester to imatinib-sensitive KCL22 cells resulted in a 2.8-fold increase in the IC_{50} value of imatinib (Fig. 3C). We also examined the effect of buthionine sulfoximine (BSO; a potent inhibitor of γ-GCS) on imatinib sensitivity of KCL22/SR cells, but failed to obtain usable results because of the severe toxicity of BSO.

Ascorbic acid reduced Nrf2/DNA complex formation by inhibiting movement of Nrf2 into nucleus

Because oxidative stress promotes movement of Nrf2 into the nucleus, it is likely that a shift in intracellular redox balance toward a reduced state inhibits movement of Nrf2 in KCL22/SR cells. To verify this hypothesis, we examined the effect of AA (a reducing reagent) on Nrf2/DNA complex formation. Peroxide levels in KCL22/SR cells were reduced by addition of 0.125 mM AA (Fig. 4A), strongly indicating that AA acts as an antioxidant. Formation of Nrf2/DNA complex in KCL22/SR cells was markedly decreased by addition of 0.125 mM AA (Fig. 4B) without any change in Nrf2 protein level in total cell lysate (Fig. 4C), suggesting that AA inhibited movement of Nrf2 into the nucleus.

Ascorbic acid restores imatinib sensitivity in KCL22/SR cells

We next examined the effects of AA on GSH synthesis and growth of KCL22/SR cells. Although the level of γ-GCS heavy subunit mRNA was not changed (data not shown), that of γ-GCSl mRNA was significantly reduced by addition of 0.125 mM AA (Fig. 5A). Simultaneously, GSH concentration in KCL22/SR cells was reduced (Fig. 5B), indicating that AA inhibited GSH synthesis. AA had no inhibitory effect on growth of KCL22/SR cells when administered alone, but combined treatment of KCL22/SR cells with imatinib and AA resulted in inhibition of cell growth (Fig. 5C). Consistent with these findings, addition of 0.125 mM AA resulted in a 50% decrease in the IC_{50} value of imatinib for KCL22/SR cells, suggesting that AA at this concentration is not directly cytotoxic but restores sensitivity of KCL22/SR cells to imatinib via, at least in part, suppression of intracellular GSH level.

Formation of Nrf2/DNA complex is increased in another imatinib-resistant cell line

To clarify whether an increase in formation of Nrf2/DNA complex occurs in imatinib-resistant cells in general or occurs only in KCL22/SR cells, we performed gel mobility shift assays using nuclear extracts of the imatinib-resistant cell lines K562/SR and KU812/SR, which were recently cloned in our lab, and their imatinib-sensitive parental strains (K562 and KU812, respectively). As shown in Figure 6, while there was no difference in the level of Nrf2/DNA complex between KU812/SR and KU812, the level of Nrf2/DNA complex was higher in K562/SR than in K562. These

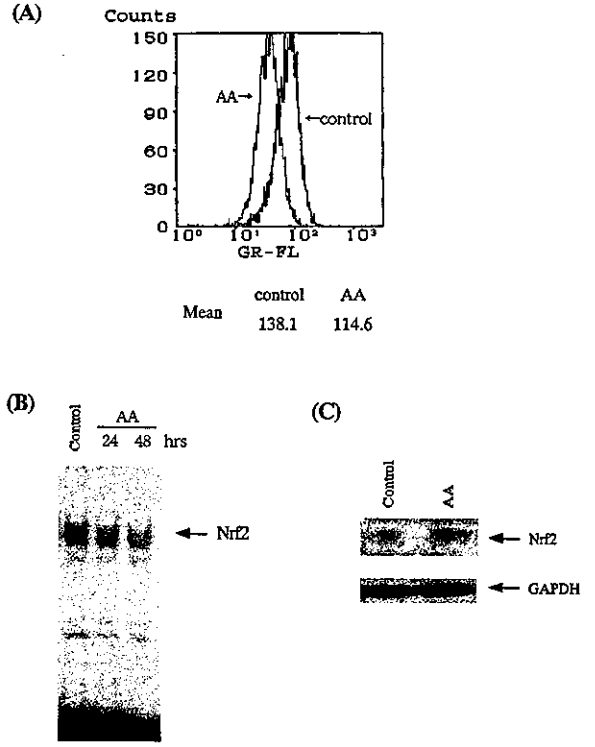

Figure 4. Effect of ascorbic acid on formation of Nrf2/DNA complex. (**A**): KCL22/SR cells were incubated with 0.125 mM ascorbic acid (AA) for 6 hours. The level of intracellular peroxides was determined by flow cytometry, as described in Materials and Methods. Decreased green fluorescence correlates with decreased peroxide levels. (**B**): KCL22/SR cells were incubated with 0.125 mM AA. The level of Nrf2/DNA complex formation at various time points was evaluated by gel mobility shift assay using oligomers corresponding to ARE. (**C**): KCL22/SR cells were cultured in the absence or presence of 0.125 mM AA for 24 hours. The levels of Nrf2 protein in total cell extracts were examined by immunoblot analysis using anti-Nrf2 antibody. The expression of glyceraldehyde-3-phosphate dehydrogenase (GAPDH) was examined as an internal control.

results suggest that induction of Nrf2 activity is involved in resistance to imatinib in some, but not all, imatinib-resistant cell lines.

Discussion

Recently, various new anti-cancer agents that target specific oncogenic molecules have been developed. Imatinib is one of the most successful of these reagents. However, a major problem with imatinib treatment is acquisition of resistance. In the present study, we used the imatinib-resistant BCR/ABL$^+$ cell line KCL22/SR to investigate the mechanisms of resistance to imatinb. KCL22/SR was cloned from the human BCR/ABL$^+$ cell line KCL/22. The IC_{50} value of imatinib for KCL22/SR is about 11.6-fold higher than that of KCL22, indicating that KCL22/SR has acquired significant resistance to imatinib [25]. Examination of KCL22/SR has revealed no mutations in the BCR/ABL gene and no increase in levels of BCR/ABL protein or P-glycoprotein. Given that the level of phosphorylated BCR/ABL protein is suppressed by imatinib treatment, these previous findings suggest that mechanisms independent of BCR/ABL activity are involved in the imatinib resistance of KCL22/SR [25]. The present results suggest that Nrf2 is involved in the imatinib resistance of KCL22/SR.

Nrf2 has been shown to regulate ARE-mediated gene expression. The present results demonstrate that formation of Nrf2/DNA complex at the ARE of the γ-GCSl gene promoter occurs at a significantly higher rate in KCL22/SR cells than in KCL22 cells (Fig. 1A). The amount of Nrf2/DNA complex was also increased in the imatinib-resistant cell line K562/SR, compared with its parental imatinib-sensitive line, K562 (Fig. 6), suggesting that this phenomenon occurs in many types of imatinib-resistant cells other than KCL22/SR cells. Consistent with these findings, the level of γ-GCSl mRNA was significantly higher in KCL22/SR cells than in KCL22 cells (Fig. 3A). The light subunit of the γ-GCS enzyme is a regulatory subunit and is important for regulation of γ-GCS activity. There was no difference in levels of γ-GCS heavy subunit (which contains a catalytic domain of γ-GCS) mRNA between KCL22/SR and KCL22 (data not shown). Nrf2-mediated induction of light subunit expression may result in upregulation of γ-GCS activity and a consequent increase in GSH synthesis (Fig. 3B). Addition of a GSH monoester to KCL22 cells resulted in an increase in the IC_{50} value of imatinib (Fig. 3C), suggesting that upregulation of GSH synthesis due to increased Nrf2 activity is involved, at least in part, in the imatinib resistance of KCL22/SR cells. Clarification of whether similar abnormalities are involved in the imatinib resistance in primary cells from imatinib-resistant leukemia patients is important, and such studies are now being carried out in our laboratory.

GSH has been shown to detoxify substances in cells via conjugation and transport out of the cell [20]. However, it is unlikely that GSH directly inactivates imatinib via conjunction in KCL22/SR cells, because imatinib still effectively suppressed BCR/ABL kinase activity in these cells. Thus, mechanisms of imatinib resistance due to GSH accumulation may involve effects on other biological functions, such as intracellular signaling. Since addition of GSH did not result in restoration of the imatinib-mediated reduction of phospho-ERK1/2 levels in KCL22 cells (data not shown), MAPK may not be involved in the mechanisms of imatinib resistance due to GSH accumulation.

The present findings strongly suggest that Nrf2 is a good molecular target for overcoming imatinib resistance. AA reduced peroxide levels (Fig. 4A) and suppressed levels of Nrf2/DNA complex at the ARE of the γ-GCSl gene promoter (Fig. 4B). Consistent with these results, treatment of KCL22/SR cells with AA resulted in reduced GSH level and enhanced sensitivity to imatinib (Fig. 5C). Although we have no clinical data on the effect of ascorbic acid in imatinib-resistant patients, an in vitro experiment showed that treatment with AA and imatinib also suppressed growth of leukemia cells from a patient with CML in BC who had relapsed during

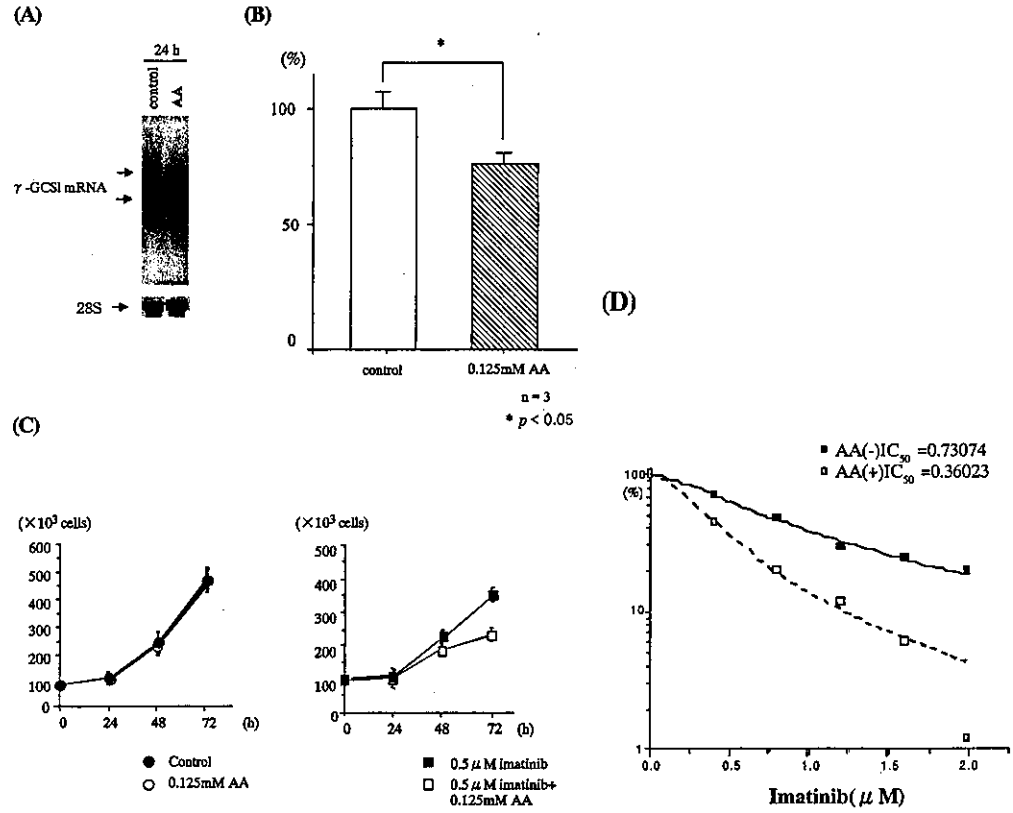

Figure 5. Effect of AA on GSH synthesis in KCL22/SR cells. **(A,B)**: KCL22/SR cells were cultured in the presence of 0.125 mM AA for 24 hours. Changes in the levels of γ-GCSl mRNA **(A)** and GSH concentration **(B)** were examined as described in Materials and Methods. **(C)**: KCL22/SR cells were incubated with or without 0.125 mM AA in the absence or presence of 0.5 μM imatinib for 72 hours. Viable cells were counted by trypan blue exclusion at various time points, as indicated in the figure. **(D)**: KCL22/SR cells were incubated in the presence of various concentrations of imatinib with or without ascorbic acid. The IC_{50} values of imatinib are shown in the figure.

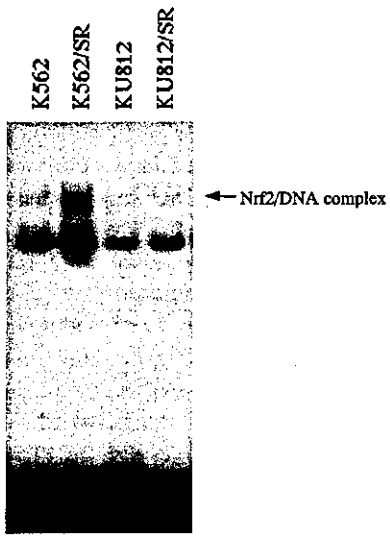

Figure 6. Formation of Nrf2/DNA complex at ARE in other imatinib-resistant cell lines. Nuclear extracts were prepared from K562, K562/SR, KU812, and KU812/SR cells. Gel mobility shift assay was performed using the end-labeled oligomers corresponding to ARE.

imatinib treatment (data not shown). We did not examine changes in Nrf2/DNA complex formation induced by AA in that case; however, it is possible that AA-induced inhibition of Nrf2 activity strengthened the effect of imatinib. It has been reported that reactive oxygen species could inhibit the activity of protein tyrosine phosphatases, resulting in the induction of protein tyrosine phosphorylation [32]. Thus, AA may also have other biological effects through phosphatase activation. Taken together, these results suggest that AA is an attractive molecular target reagent for overcoming resistance to imatinib in some imatinib-resistant CML cells.

Acknowledgments

This work was supported in part by Grants-in-Aid from the Ministry of Education, Culture, Sports, Science and Technology, Japan. We wish to thank Ms. E. Yamakawa for her help in preparation of the manuscript.

References

1. Druker BJ, Talpaz M, Resta DJ, et al. Efficacy and safety of a specific inhibitor of the BCR-ABL tyrosine kinase in chronic myeloid leukemia. N Engl J Med. 2001;344:1031–1037.

2. Druker BJ, Sawyers CL, Kantarjian H, et al. Activity of a specific inhibitor of the BCR/ABL tyrosine kinase in the blast crisis of chronic myeloid leukemia and acute lymphoblastic leukemia with the Philadelphia chromosome. N Engl J Med. 2001;344:1038–1042.
3. Sawyers CL, Hochhaus A, Feldman E, et al. Imatinib induces hematologic and cytogenetic responses in patients with chronic myelogenous leukemia in myeloid blast crisis: results of a phase II study. Blood. 2002;99:3530–3539.
4. le Coutre P, Tassi E, Varella-Garcia M, et al. Induction of resistance to the Abelson inhibitor STI571 in human leukemic cells through gene amplification. Blood. 2000;95:1758–1766.
5. Weisberg E, Griffin JD. Mechanism of resistance to the ABL tyrosine kinase inhibitor STI571 in BCR/ABL-transformed hematopoietic cell lines. Blood. 2000;95:3498–3505.
6. Mahon FX, Deininger MW, Schultheis B, et al. Selection and characterization of BCR-ABL$^+$ cell lines with differential sensitivity to the tyrosine kinase inhibitor STI571: diverse mechanisms of resistance. Blood. 2000;96:1070–1079.
7. Gorre ME, Mohammed M, Ellwood K, et al. Clinical resistance to STI571 cancer therapy caused by BCR-ABL gene mutation of amplification. Science. 2001;293:876–880.
8. Branford S, Rudzki Z, Walsh S, Grigg A, Arihur C, Taylor K. High frequency of point mutations clustered within the adenosine triphosphate–binding region of BCR/ABL in patients with chronic myeloid leukemia or Ph$^+$ acute lymphoblastic leukemia who develop imatinib (STI571) resistance. Blood. 2002;99:3472–3475.
9. Gambacorti-Passerini C, Barni R, le Coutre P, et al. Role of α1 acid glycoprotein in the in vivo resistance of human BCR-ABL$^+$ leukemic cells to the Abl inhibitor STI571. J Natl Cancer Inst. 2000;92:1641–1650.
10. Venugopal R, Jaiswal AK. Nrf1 and Nrf2 positively and c-Fos and Fra1 negatively regulate the human antioxidant response element–mediated expression of NAD(P)H:quinone oxidoreductase1 gene. Proc Natl Acad Sci U S A. 1996;93:14960–14965.
11. Venugopal R, Jaiswal AK. Nrf2 and Nrf1 in association with Jun proteins regulate antioxidant response element–mediated expression and coordinated induction of genes encoding detoxifying enzymes. Oncogene. 1998;17:3145–3156.
12. Itoh K, Wakabayashi N, Katoh Y, et al. Keap1 represses nuclear activation of antioxidant responsive elements by Nrf2 through binding to the amino-terminal Neh2 domain. Genes Dev. 1999;13:76–86.
13. Itoh K, Chiba T, Takahashi S, et al. An Nrf2/small Maf heterodimer mediates the induction of phase II detoxifying enzyme genes through antioxidant response elements. Biochem Biophys Res Commun. 1997; 236:313–322.
14. Ishii T, Itoh K, Takahashi S, et al. Transcription factor Nrf2 coordinately regulates a group of oxidative stress-inducible genes in macrophages. J Biol Chem. 2000;275:16023–16029.
15. Richman PG, Meister A. Regulation of γ-glutamyl-cysteine synthetase by nonallosteric feedback inhibition by glutathione. J Biol Chem. 1975; 250:1422–1426.
16. Meister A. Glutathione metabolism. Methods Enzymol. 1995;251:3–7.
17. Filomeni G, Rotilio G, Ciriolo MR. Glutathione disulfide induces apoptosis in U937 cells by a redox-mediated p38 MAP kinase pathway. FASEB J. 2003;17:64–66.
18. Kong AN, Yu R, Lei W, Mandlekar S, Tan TH, Ucker DS. Differential activation of MAPK and ICE/Ced-3 protease in chemical-induced apoptosis: the role of oxidative stress in the regulation of mitogen-activated protein kinases (MAPKs) leading to gene expression and survival or activation of caspases leading to apoptosis. Restor Neurol Neurosci. 1998;12:63–70.
19. Haddad JJ. Redox regulation of pro-inflammatory cytokines and IκB-α/NF-κB nuclear translocation and activation. Biochem Biophys Res Commun. 2002;296:847–856.
20. Hayes JD, Pulford DJ. The glutathione S-transferase supergene family: regulation of GST and the contribution of the isoenzymes to cancer chemoprotection and drug resistance. Crit Rev Biochem Mol Biol. 1995;30:445–600.
21. Iida T, Mori E, Mori K, et al. Co-expression of γ-glutamylcysteine synthetase sub-units in response to cisplatin and doxorubicin in human cancer cells. Int J Cancer. 1999;82:405–411.
22. Takemura H, Urasaki Y, Yoshida A, Fukushima T, Ueda T. Simultaneous treatment with 1-β-D-arabinofuranosylcytosine and daunorubicin induces cross-resistance to both drugs due to a combination-specific mechanism in HL60 cells. Cancer Res. 2001;61:172–177.
23. Moinova HR, Mulcahy RT. An electrophile responsive element (EpRE)regulates β-naphthoflavone induction of the human γ-glutamylcysteine synthetase regulatory subunit gene. Constitutive expression is mediated by an adjacent AP-1 site. J Biol Chem. 1998;273:14683–14689.
24. Kubonishi I, Miyoshi I. Establishment of a Ph1 chromosome–positive cell line from chronic myelogenous leukemia in blast crisis. Int J Cell Cloning. 1983;1:105–117.
25. Ohmine K, Nagai T, Tarumoto T, et al. Analysis of gene expression profiles in an imatinib-resistant cell line, KCL22/SR. Stem Cells. 2003; 21:315–321.
26. Anderson ME, Levy EJ, Meister A. Preparation and use of glutathione monoesters. Methods Enzymol. 1994;234:492–499.
27. Nagai T, Tarumoto T, Miyoshi T, et al. Oxidative stress is involved in hydroxyurea-induced erythroid differentiation. Br J Haematol. 2003; 121:657–661.
28. Chomczynski P, Sacchi N. Single-step method of RNA isolation by acid guanidinium thiocyanate-phenol-chloroform extraction. Anal Biochem. 1987;162:156–159.
29. Nagai T, Harigae H, Ishihara H, et al. Transcription factor GATA-2 is expressed in erythroid, early myeloid, and CD34$^+$ human leukemia–derived cell lines. Blood. 1994;84:1074–1084.
30. Lassar AB, Davis RL, Wright WE, et al. Functional activity of myogenic HLH proteins requires hetero-oligomerization with E12/E47-like proteins in vivo. Cell. 1991;66:305–315.
31. Nagai T, Harigae H, Furuyama K, et al. 5-aminolevulinate synthase expression and hemoglobin synthesis in a human myelogenous leukemia cell line. J Biochem (Tokyo). 1997;121:487–495.
32. Sattler M, Verma S, Shrikhande G, et al. The BCR/ABL tyrosine kinase induces production of reactive oxygen species in hematopoietic cells. J Biol Chem. 2000;275:24273–24278.

THE JOURNAL OF GENE MEDICINE
J Gene Med 2004; 6: 288–299.
Published online 28 January 2004 in Wiley InterScience (www.interscience.wiley.com). **DOI:** 10.1002/jgm.490

RESEARCH ARTICLE

In situ generation of pseudotyped retroviral progeny by adenovirus-mediated transduction of tumor cells enhances the killing effect of HSV-*tk* suicide gene therapy *in vitro* and *in vivo*

Takashi Okada,[1]* Natasha J. Caplen,[2] W. Jay Ramsey,[3] Masafumi Onodera,[4] Kuniko Shimazaki,[5] Tatsuya Nomoto,[1] Rahim Ajalli,[1] Oliver Wildner,[6] John Morris,[7] Akihiro Kume,[1] Hirofumi Hamada,[8] R. Michael Blaese,[9] Keiya Ozawa[1]

[1]*Division of Genetic Therapeutics, Center for Molecular Medicine, Jichi Medical School, Tochigi, Japan*
[2]*Medical Genetics Branch, National Human Genome Research Institute, National Cancer Institute, NIH, Bethesda, MD, USA*
[3]*Link Pharmaceuticals, Ames, IA, USA*
[4]*Department of Hematology, Institute of Basic Medical Sciences, University of Tsukuba, Japan*
[5]*Department of Physiology, Jichi Medical School, Tochigi, Japan*
[6]*Abt. f. Mol. u. Med. Virologie, Ruhr-Universit, Bochum, Germany*
[7]*Metabolism Branch, National Cancer Institute, NIH, Bethesda, MD, USA*
[8]*Biomolecular Medical Section, Biomedical Research Center, Sapporo Medical University, Sapporo, Japan*
[9]*PreGentis, Newtown, PA, USA*

*Correspondence to: Takashi Okada, Division of Genetic Therapeutics, Center for Molecular Medicine, Jichi Medical School, 3311-1 Yakushiji, Minami-kawachi, Tochigi 329-0498, Japan. E-mail: tokada@jichi.ac.jp

Received: 3 March 2003
Revised: 24 July 2003
Accepted: 2 August 2003

Abstract

Background Hybrid adeno-retroviral vector systems utilize the high efficiency of adenovirus transduction to direct the *in situ* production of retroviral progeny. In this study, we show that a single-step transduction of glioma cells with trans-complementing hybrid adeno-retroviral vectors effectively turns these cells into retrovirus vector-producing cells, which in turn facilitates the transduction of adjacent cells.

Methods We have adapted the adeno-retroviral hybrid viral vector system to enhance the ganciclovir (GCV) killing of glioma cells following transfer of the herpes simplex virus thymidine kinase (HSV-*tk*) gene. To assess the effect of the *in situ* production of retroviral vectors on the transduction efficiency of glioma cells, 9L cells were transduced with adeno-retroviral hybrid vectors that separately express a retroviral genome (AVC2.GCEGFP or AVC2.GCTK) and retroviral packaging proteins (AxTetGP and AxTetVSVG). The generation of an integrated HSV-*tk* provirus by trans-complementation of the adeno-retroviral vectors was verified by analysis of the flanking retroviral LTR sequences. Tumors established on *nu/nu* mice were injected with the viruses followed by intraperitoneal injections of either PBS or GCV. We also estimated the copy numbers of the HSV-*tk* transgene present in the tumors of the treated mice. To determine the expression pattern of the HSV-*tk* transcripts within a tumor, *in situ* hybridization analysis was performed using an RNA probe specific for HSV- *tk*.

Results The co-transduction of rat 9L glioma cells with AVC2.GCEGFP together with vectors expressing packaging proteins of retroviruses increased the transduction efficiency. Transduction with AVC2.GCTK together with packaging vectors increased the *in vitro* sensitivity of cells to the pro-drug GCV by one log compared with control cells that were incapable of generating retrovirus. *In vivo*, the injection of established subcutaneous 9L tumors on athymic mice with a combination of AVC2.GCTK and packaging vectors followed by GCV treatment resulted in complete tumor regression in 50% of tumors at day 22, while no tumor regression was observed in control animals. Retroviral sequences diagnostic of 3′ LTR reduplication *in vivo* were detected in genomic DNA extracted from the transduced tumors, indicating pro-viral integration of the retroviral genome derived from the adeno-retroviral hybrid vector. Furthermore, the relative copy number of the HSV-*tk* gene in tumors treated with the adeno-retroviral vectors was up to ~250-fold higher than in control tumors. *In situ* hybridization suggested dispersion of the HSV-*tk*

product across a wider area of the tumor than in control tumors, which indicates the spread of the *in situ* generated retroviruses.

Conclusions Although the efficacy of this system has to be evaluated in orthotopic models, our observations suggest that this hybrid adeno-retroviral vector system could improve the suicide gene therapy of tumors. Copyright © 2004 John Wiley & Sons, Ltd.

Keywords suicide gene therapy; adeno-retroviral hybrid vector; *in situ* generation; glioma; HSV-*tk*

Introduction

When tumor cells that have been transformed with the herpes simplex virus thymidine kinase (HSV-*tk*) gene are treated with the pro-drug ganciclovir (GCV), they regress [1]. However, the clinical benefit of this cancer gene therapy system is limited due to the poor efficiency of gene transfer [2]. To improve the therapeutic potential of this system, it is necessary to enhance the efficiency of the delivery of a therapeutic gene *in vivo* as well as to increase the stability of the expression of the gene.

We and others have previously described hybrid vector systems that use adenoviral vectors to deliver retroviral vector and packaging proteins into cells [3–9]. These systems benefit from the efficient gene transfer characteristics of adenoviral vectors as well as from the stable and long-term gene expression that is typical of retroviral vectors. The initial co-transduction of such adeno-retroviral hybrid vectors results in the transient production of recombinant retrovirus particles that then subsequently transduce neighboring cells. Adenovirus vectors expressing trans-complementing genes for retroviral proteins and retroviral vector RNAs have been successfully used for the *in situ* transduction of tumor cells [3,7].

We describe here an improved adeno-retroviral vector system that efficiently produces pseudotyped retroviral vectors. To simplify the construction of the chimeric vector carrying the retroviral genome, the directional ligation technique with the DNA–protein complex was employed [10]. We show that our adeno-retroviral packaging system can be used to rescue an integrated retroviral provirus in tumor cells and to enhance the therapeutic gene expression in glioma cells. In addition, we demonstrate that an adeno-retroviral HSV-*tk* vector system coupled with GCV enhances GCV-mediated killing of glioma cells both *in vitro* and *in vivo*. This suggests that this strategy produces sufficient levels of vectors *in situ* for the killing of solid tumors.

Materials and methods

Plasmid construction

The hybrid adeno-retroviral vector plasmid pAVC2.GCE-GFP was constructed as follows. The 3′ long terminal repeat (LTR) (*Cla* I-*Nde* I fragment) of the Molony murine leukemia virus (MMLV)-based retroviral vector pGCsap was replaced with the 3′ LTR (*Cla* I-*Nde* I fragment) of the myeloproliferative sarcoma virus (MPSV) to form pGCsapM. To generate pGCsapMEGFP, the *Nco* I-*Not* I fragment from pEGFP-N1 (Clontech Laboratories, Palo Alto, CA, USA) containing cDNA encoding the enhanced green fluorescent protein (EGFP) was cloned into *Nco* I-*Not* I-digested pGCsapM. This ensured that the EGFP translational initiation site was precisely located at the *env* translational start site found in the wild-type MMLV retrovirus. The retroviral vector GCsapMEGFP cassette was then cloned as an *Asc* I–*Xba* I-fragment into *Asc* I–*Xba* I-digested pAVC2.LXSN [5], from which the LXSN retroviral vector genome had been removed, to generate pAVC2.GCEGFP (Figure 1A).

The hybrid adeno-retroviral vector plasmid pAVC2.GC-TK was derived from pGCsam [11]. The full length coding region of the HSV-*tk* cDNA contained in the *Spe* I-*Cla* I fragment from pAVS6TK [12] was subcloned into pBluescript SK (+) and then cloned as a *Not* I–*Cla* I fragment into *Not* I–*Cla* I-digested pGCsam, which generated pGCsamTK. To construct pAVC2.GCTK (Figure 1A), the retroviral vector GCsamTK cassette was cloned as an *Asc* I–*Xba* I fragment into *Asc* I–*Xba* I-digested AVC2.LXSN.

Generation of adenovirus vectors

The recombinant hybrid adeno-retroviruses AVC2.GCE-GFP and AVC2.GCTK were generated using the mutant adenovirus type 5, dl327 [13]. A DNA–protein complex of dl327 was prepared as described previously [10]. The dl327 DNA–protein complex was digested with *Cla* I and *Bst* Z17 and treated with bacterial alkaline phosphatase (LTI, Grand Island, NY, USA) at 37 °C for 30 min. The enzymes were removed by three cycles of dilution with TE (pH 8.0) followed by concentration by using a Centricon YM-100 column according to the manufacturer's instructions (Amicon, Beverly, MA, USA). The AVC2.GCEGFP and AVC2.GCTK cassettes were excised from their respective plasmids (pAVC2.GCEGF and pAVC2.GCTK) by *Rca* I and *Bst* Z17 digestion and purified by agarose gel electrophoresis (QIAquick gel extraction kit; Qiagen, Hilden, Germany). The purified

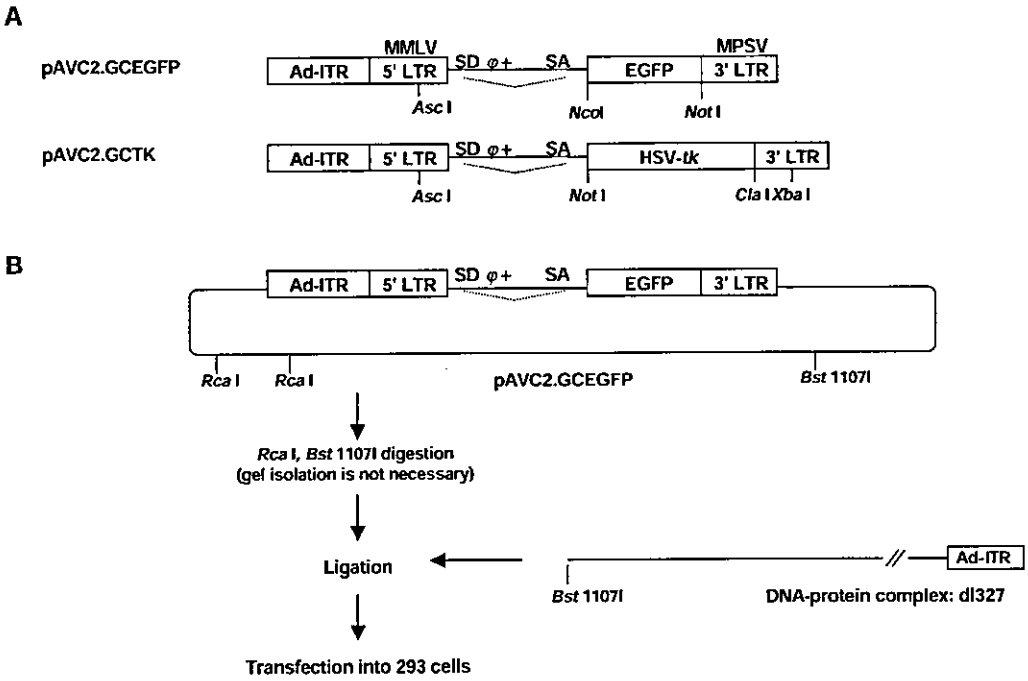

Figure 1. Schematic representation of the adeno-retroviral hybrid vectors used in this study. (A) The adeno-retroviral hybrid vector plasmids containing retroviral vector genomes expressing either GFP (AVC2-GCEGFP) or HSV-*tk* (AVC2-GCTK). SD, splice donor; SA, splice acceptor. (B) Cloning of recombinant adeno-retroviral hybrid vectors using directed ligation of a linearized vector plasmid into a DNA–protein complex in a single step without homologous recombination

fragments were mixed with 0.2 μg of *Cla* I- and *Bst* Z17-digested dl327 DNA–protein complex (Figure 1B) at a molar ratio of 3 : 1 and ligated with 5 Weiss U of T4 DNA ligase (New England Biolabs, Beverly, MA, USA) in a volume of 10 μl overnight at 9 °C. The ligated samples were desalted by using a Centricon YM-100 column and transfected into 293 cells by calcium phosphate co-precipitation, after which the cells were overlaid with agar as previously described [14]. The infectivity of the ligated DNA–protein complex was approximately 10 plaque-forming units/μg of DNA–protein complex for both vectors. Virus plaques were isolated and expanded in 293 cells. All viruses screened by PCR for the presence of the inserted retrovirus vector genome were positive. A control adenovirus vector AVC2.null with no expression gene cassette was constructed and propagated as described before [10]. The adenoviruses AxTetGP and AxTetVSVG expressing the MMLV gag-pol and the G protein of vesicular stomatitis virus (VSV-G) envelope protein, respectively, have been described previously [15]. The expression of the gag-pol and VSV-G proteins is under the control of the transcriptional regulator reverse Tet-controlled transactivator (rtTA) that is supplied by the adenoviral vector AV-rtTA [7]. These adenoviral vectors were propagated and purified as described previously [14].

Cell lines

The amphotropic retroviral vector producer cell line FLYA13 [16], the rat glioma cell line 9L [17], the human glioma cell line D54 [18], and the human embryonic kidney cell line 293 [19] were cultured in Dulbecco's modified Eagle's medium (DMEM high glucose; 4.5 g/l, Life Technologies, Gaithersburg, MD, USA) supplemented with 10% fetal bovine serum (FBS, Life Technologies), 100 units/ml penicillin, 100 μg/ml streptomycin, and 2 mM glutamine at 37 °C, 10% CO_2. To express the transgene from AxTetGP and AxTetVSVG, the cell culture medium was supplemented with 1 μg/ml doxycycline (Sigma, St. Louis, MO, USA). The GFP reporter cell line D54GFPneo was established by transfecting the retroviral expression plasmid pGC-GFP-loxP-EN [20] into D54 cells by calcium phosphate co-precipitation [21] followed by selection of independent GFP-positive colonies with 0.5 mg/ml G418 (Life Technologies).

Viral transductions

The cells were transduced with adenoviruses for 3 h at a variety of multiplicities as described for each experiment. The cells were washed with growth medium supplemented with 1 μg/ml of human serum γ-globulin (Miles Research Products Division, Elkhart, IN, USA) as a source of neutralizing antibody against adenovirus (these washes significantly reduce the carryover of residual adenoviral vectors in newly synthesized retroviral supernatants [5]). Finally, growth medium supplemented with human serum γ-globulin (1 μg/ml) and doxycycline (1 μg/ml) was added to each flask.

Putative retroviral-containing supernatants were harvested at the indicated time and centrifuged at 700 *g*, 4 °C,

filtered (0.45 μm), aliquotted and stored at −80 °C. For retroviral transduction, target cells were plated in 6-well plates at 5×10^4 cells per well and incubated overnight at 37 °C in 5% CO_2. Duplicate retroviral transductions were conducted at 37 °C by plating 2 ml of undiluted viral supernatant supplemented with polybrene (8 μg/ml) for 48 h.

FACS analysis

Fluorescence-activated cell sorting (FACS) analysis was performed on a FACSCalibur (Becton Dickinson, San Jose, CA, USA) equipped with an argon gas laser. A standard band-pass filter was used to determine green fluorescence intensity. Approximately 5×10^4 cells from each sample were analyzed. The FL1 signal was acquired in logarithmic mode, and the data were analyzed with CellQuest software (Becton Dickinson).

RNA dot blot analysis

To estimate the retroviral supernatant titers, RNA dot blot analysis was performed as described previously [22]. Briefly, nylon membranes (Hybond N^+; Amersham Life Sciences, Arlington Heights, IL, USA) were soaked for 10 min in 1× SSC (0.15 M NaCl, 0.015 M sodium citrate) and placed onto a manifold dot blot apparatus (Schleicher & Schuell Inc., Keene, NH, USA). To avoid detection of the adenovirus DNA, supernatant (180 μl) without denaturing procedure was transferred onto nylon membranes using the manifold dot blot apparatus and vacuum suction. The membranes were cross-linked by UV and hybridized with a MMLV *psi* cDNA probe that had been randomly labeled with [α^{32}P] dCTP (Megaprime DNA labeling systems, Amersham Life Sciences). The membranes were subjected to phosphoimager analysis, and dot blot densities were measured with a Bio imaging analyzer (BAS1500; Fuji Photo Film Co., Ltd., Tokyo, Japan). Dot densities were expressed as relative pixel intensity and retroviral titers were determined by comparison with the known expression titer in a supernatant of the retrovirus vector LASN [23].

Adenovirus detection in the retroviral supernatants

To assay for the presence of biologically active adenovirus in the retroviral supernatants, 293 cells (1×10^4) were incubated with 200 μl of samples for 72 h. The presence of adenovirus was assessed by monitoring for evidence of cytopathic effects and the detachment of the cells 2 weeks later.

GCV sensitivity assay

The killing effect of GCV (Syntex, Palo Alto, CA, USA) was measured by ^{3}H-thymidine incorporation [24]. Briefly, 5×10^4 cells were cultured in 96-well flat-bottomed microtiter plates in the presence of varying concentrations (0–50 μM) of GCV. After 42 h the cells were pulsed with 0.25 μCi per well of ^{3}H-thymidine (Amersham International, Bucks, UK) and harvested 6 h later. The effect of GCV on tumor cell proliferation is expressed as a percentage of the thymidine incorporation found in the identical cultures not treated with GCV.

Molecular analysis

To confirm the integration of a retrovirus vector genome rescued by trans-complementation of the hybrid vectors, PCR analysis was conducted with high molecular weight DNA extracted from the target cells 14 days post-transduction (DNA extraction kit, Qiagen Inc.). A PCR-amplified DNA product (560 bp) was extended from the 5′ LTR or the 3′ LTR of the retroviral vector (sense primer 5′ AGGGCCAAGAACAGATGAGACAGC 3′) to a region downstream of the 5′ LTR (antisense primer: 5′ GTACAGACGCAGGCGCATAACATC 3′). Conversion of the 3′ LTR to the 5′ LTR after provirus integration was confirmed by digestion with *Xba* I. The PCR product was transferred to a nylon membrane (Hybond N^+; Amersham Life Sciences) by the capillary transfer method.

Vector treatment *in vivo*

Athymic female BALB/c *nu/nu* mice (Clea Japan, Tokyo, Japan) were inoculated subcutaneously with 9L cells (3×10^6 cells) in 100 μl Hank's balanced salt solution containing 25% (v/v) basement membrane matrix (Matrigel; BD Biosciences, Franklin Lakes, NJ, USA). The tumors were allowed to grow *in vivo* to an average volume of 70 mm^3 (tumor volumes were calculated as $a \times b^2 \times 0.5$ where a is the length and b is the width of the tumor in millimeters). The established subcutaneous tumors were injected with a control vector (group 1, AVC2.null), a therapeutic vector (group 2, AVC2.GCTK), a combination of vectors without the *gag-pol* expressing vector (group 3, AVC2.GCTK, AVC2.null, AxTetVSVG, and AV-rtTA), or the complete set of trans-complementing adenoviral vectors that rescues the retrovirus (group 4, AVC2.GCTK, AxTetGP, AxTetVSVG, and AV-rtTA). In each group, 1.0×10^9 plaque-forming units (pfu) of each virus were administered. Viruses were injected at four sites in each tumor with 100 μl of the virus solution in total. The animals received doxycycline as a 10 mg/ml solution in 5% sucrose via their water bottles for a period of 3 days starting 24 h after virus administration. When the tumor volume reached an average volume of 100 mm^3, the tumor-bearing animals were treated with an intraperitoneal injection of GCV at 30 mg/kg or phosphate-buffered saline (PBS) twice a day for 14 consecutive days. Tumors with an average volume of 100 mm^3 require more than 2.0×10^9 pfu of HSV-*tk* expression adenovirus vector for their complete

elimination [12]. Tumor growth was monitored two to three times a week by measuring two perpendicular tumor diameters using calipers. The total observation time was 2 months after the virus injection. Animals with tumors larger than 1 cm in diameter were euthanized. Tumor elimination that continued for more than 4 weeks was considered to indicate complete regression.

Determination of HSV-*tk* transgene copy number

To estimate the amplified copy number of the transgene caused by the production of retroviral progeny, PCR analysis was conducted on high molecular weight DNA extracted from tumors (DNA extraction kit, Qiagen Inc.). Using pAVS6TK [12] as a standard, an HSV-*tk*-specific nucleotide sequence (nucleotides +418 to +737) was amplified by PCR. Primers were chosen with the assistance of the computer program Primer Express (Perkin-Elmer Applied Biosystems, Foster City, CA, USA). We performed BLAST searches against dbEST and nr (the non-redundant set of GenBank, EMBL, and DDBJ database sequences) to confirm the total gene specificity of the nucleotide sequences chosen as primers. The specificity of the primer sets was confirmed by sequencing the PCR amplification products cloned into the pGEM-T vector (Promega, Madison, WI, USA). Quantitative values were obtained from the threshold cycle (*Ct*) number that indicated exponential amplification of the PCR product (ABI PRISM 7700 sequence detection system; Applied Biosystems, Foster City, CA, USA). To normalize each sample, we also quantified the copy number of the *GAPDH* gene. The relative target gene copy number was also normalized with a calibrator (tumors treated with AVC2GCTK alone). The final result, expressed as *N*-fold differences in target gene copy number relative to the GAPDH gene and the calibrator, was determined by the following formula: $N\text{target} = 2^{\text{correctedΔCt(GAPDH–TK)}}$. *Ct* values of the sample were determined by subtracting the average *Ct* value of the target gene from the average *Ct* value of the *GAPDH* gene.

In situ hybridization

Tumors from mice subjected to intratumoral injection with adenovirus along with intraperitoneal PBS treatment were removed 14 days after the injection and *in situ* hybridization was performed using an antisense RNA probe specific for the HSV-*tk* transcripts. Tissue specimens from subcutaneous tumors were fixed for 12 h in 4% paraformaldehyde at 4 °C, cut into 30-μm sections and mounted on APS-coated slides. Using pAVS6TK [12] as a template, an HSV-*tk*-specific nucleotide sequence (nucleotides +418 to +737) was amplified by PCR and cloned into pGEM-T vector (Promega). The HSV-*tk* RNA probes were synthesized and labeled with digoxigenin (DIG)-labeled deoxyuridine triphosphate by using a DIG RNA-labeling kit (F. Hoffmann-La Roche Ltd, Basel, Switzerland) according to the manufacturer's instructions. A DIG-labeled antisense RNA probe was obtained by using DIG RNA labeling mixture with a *Spe* I-cut linearized template and T7 RNA polymerase. Similarly, a sense probe was prepared for negative control experiments by using an *Nco* I-digested template and SP6 RNA polymerase with the DIG RNA labeling mixture.

The 30-μm tumor sections were pretreated with 100 μg/ml proteinase K at 37 °C for 20 min. These sections were rinsed with 2 mg/ml glycine and then incubated with hybridization buffer containing 100 ng of labeled RNA probe in a moist chamber at 42 °C overnight. After hybridization, the sections were washed in 1 × SSC for 10 min at room temperature, 0.2 × SSC for 20 min at 42 °C, 2 × SSC for 2 min at room temperature, and digested with 10 μg/ml RNase A at 37 °C for 20 min. The sections were incubated in 0.5% blocking reagent for 60 min and then in a 1 : 100 dilution of alkaline phosphatase conjugated anti-DIG antibody for 60 min in a moist chamber, followed by rinsing with Tris-buffered saline. The alkaline phosphatase reaction was visualized with 5-bromo-4-chloro-3-indolyl phosphate and nitroblue tetrazolium. The sections were counterstained with methylgreen and coverslipped for light microscopy.

Results

Adeno-retroviral hybrid vectors can rescue an integrated retroviral genome from human glioma cells

To determine if an integrated retroviral genome could be rescued from glioma cells by use of our adeno-retroviral hybrid system, a human glioma cell line harboring a retroviral vector expressing GFP (D54GFPneo) was infected with a combination of adenoviral vectors that express proteins required for retroviral packaging proteins. Two trans-complementing adeno-retroviruses were used. AxTetGP expresses the MMLV gag-pol and AxTetVSVG expresses the VSV-G, which acts as the retrovirus envelope protein. In addition, a third adenovirus (AV-rtTA) was employed to regulate the expression of these viruses. As a control system in which retrovirus production does not occur, the AxTetGP virus was replaced by the non-expressing adenovirus vector AVC2null. Cells were infected with the appropriate adenovirus vectors for 3 h at various multiplicities of infection (MOIs). Free adenovirus was removed by washing cells with medium supplemented with human γ-globulin. Putative retrovirus-containing supernatants were harvested 48 h post-adenoviral transduction and used to transduce rat glioma 9L cells (Figure 2). Analysis of the 9L cells showed significant levels of GFP 2 days after the initiation of transduction (Figure 2A). In contrast, target 9L cells exposed to supernatants obtained from D54GFPneo cells transduced with the null adenoviral

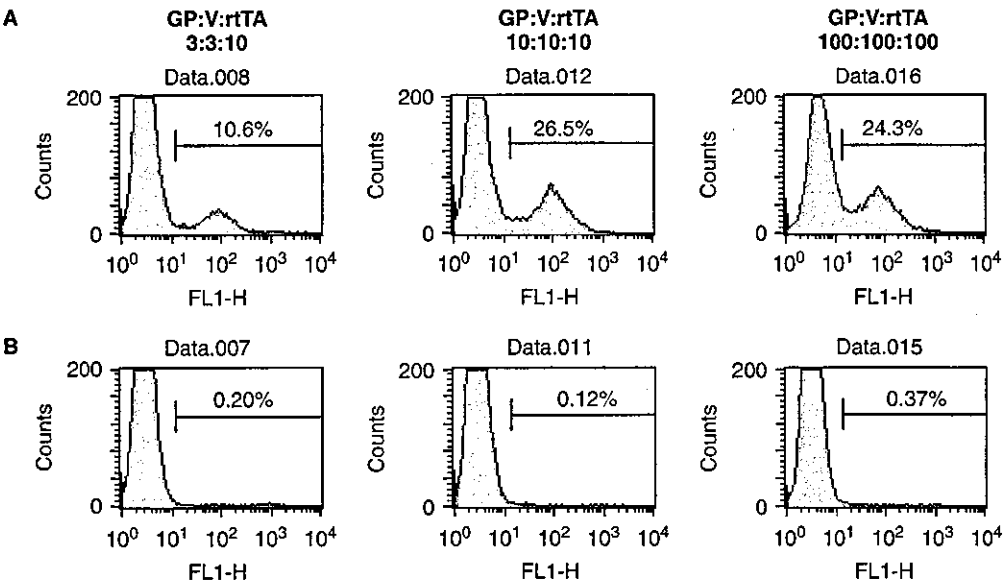

Figure 2. Rescue of an integrated GFP-expressing retroviral vector in 9L glioma cells by transduction with trans-complementing adeno-retroviral hybrid vectors. Putative retrovirus-containing supernatants were obtained from a human glioma cell line carrying an integrated retrovirus (D54GFPneo) following transduction with trans-complementing adeno-retroviral hybrid vectors at various MOIs. The putative retroviral supernatants were used to transduce 9L glioma cells so that the production of progeny retroviruses carrying the integrated GFP gene could be detected. (A) FACS analysis of 9L cells exposed to supernatants from D54GFPneo cells that had been transduced with all of the adeno-retroviral vectors required for the generation of a retrovirus, namely, AxTetGP (GP), AxTetVSVG (V), and AV-rtTA (rtTA). (B) FACS analysis of 9L cells exposed to supernatants from D54GFPneo cells transduced with all of the adeno-retroviral vectors except for the retroviral gag-pol-expressing vector, which was replaced by the control AVC2.null vector

vector plus the adenoviral vectors expressing the VSV-G envelope protein and the rtTA showed little or no GFP expression (Figure 2B). The percentage of target cells that were transduced reached a plateau when an MOI of 10 was used for each of the input adenoviruses. No biologically active adenovirus was detected in any of the supernatants.

In situ transduction efficiency of the adeno-retroviral hybrid vector system in glioma cells

To assess the effect of the *in situ* production of retroviral vector on the transduction efficiency of glioma cells, 9L cells were transduced with adeno-retroviral hybrid vectors expressing a retroviral genome (AVC2.GCEGFP) together with all of the retroviral packaging proteins (AxTetGP, AxTetVSVG, and AV-rtTA). Four days after the adenoviral transduction, a higher percentage of the cells were GFP-positive when they had been exposed to all of the trans-complementing adeno-retroviral vectors compared with cells exposed to AVC2.GCEGFP alone or when AxTetGP was replaced by the non-expressing adenoviral vector AVC2.null (Figure 3A). To confirm the long-term transgene expression from the retrovirus progeny generated by the adeno-retroviral vectors, we compared 9L cells transduced by all of the required adeno-retroviral hybrid viruses with those transduced by the control vector combination (AVC2.GCEGFP, AVC2.null, AxTetVSVG, and AV-rtTA). These cells were mixed with non-infected cells at a ratio of 10% transduced cells to 90% non-transduced cells and passaged every 7 days. Two weeks after the transduction, GFP reporter gene persistence and expression were analyzed by fluorescent microscopy. The GFP-positive cells from the group infected with AVC2.GCEGFP, AxTetGP, AxTetVSVG, and AV-rtTA were present in a clustered outgrowth after long-term culture, suggesting local retroviral spread and clonal origin (data not shown). This was in contrast to the cells infected with the control combination of adenoviruses (AVC2.GCEGFP, AVC2null, AxTetVSVG, and AV-rtTA), which showed attenuated GFP expression.

To determine how long cells can produce retrovirus after being infected with the vectors, a time course experiment was performed. The 9L cells were infected with all of the required adeno-retroviral hybrid viruses (AVC2.EGFP, AxTetGP, AxTetVSVG, and AV-rtTA) at an MOI of 3 in the presence of doxycycline. The titers increased and reached nearly 4×10^5 TU/ml by day 2, were maintained at similar levels until day 4, and then decreased (Figure 3B). At day 6, retrovirus production was still observed at a titer of 9×10^4 TU/ml. Thus, infected 9L cells continued to sustain retrovirus production for at least 6 days post-infection. The retention of transgene expression over time in infected cells was determined by evaluating the percentage of EGFP-positive cells by FACS analysis. The percentage of EGFP-positive cells increased over time, while the control group reached plateau at day 4 (Figure 3C).

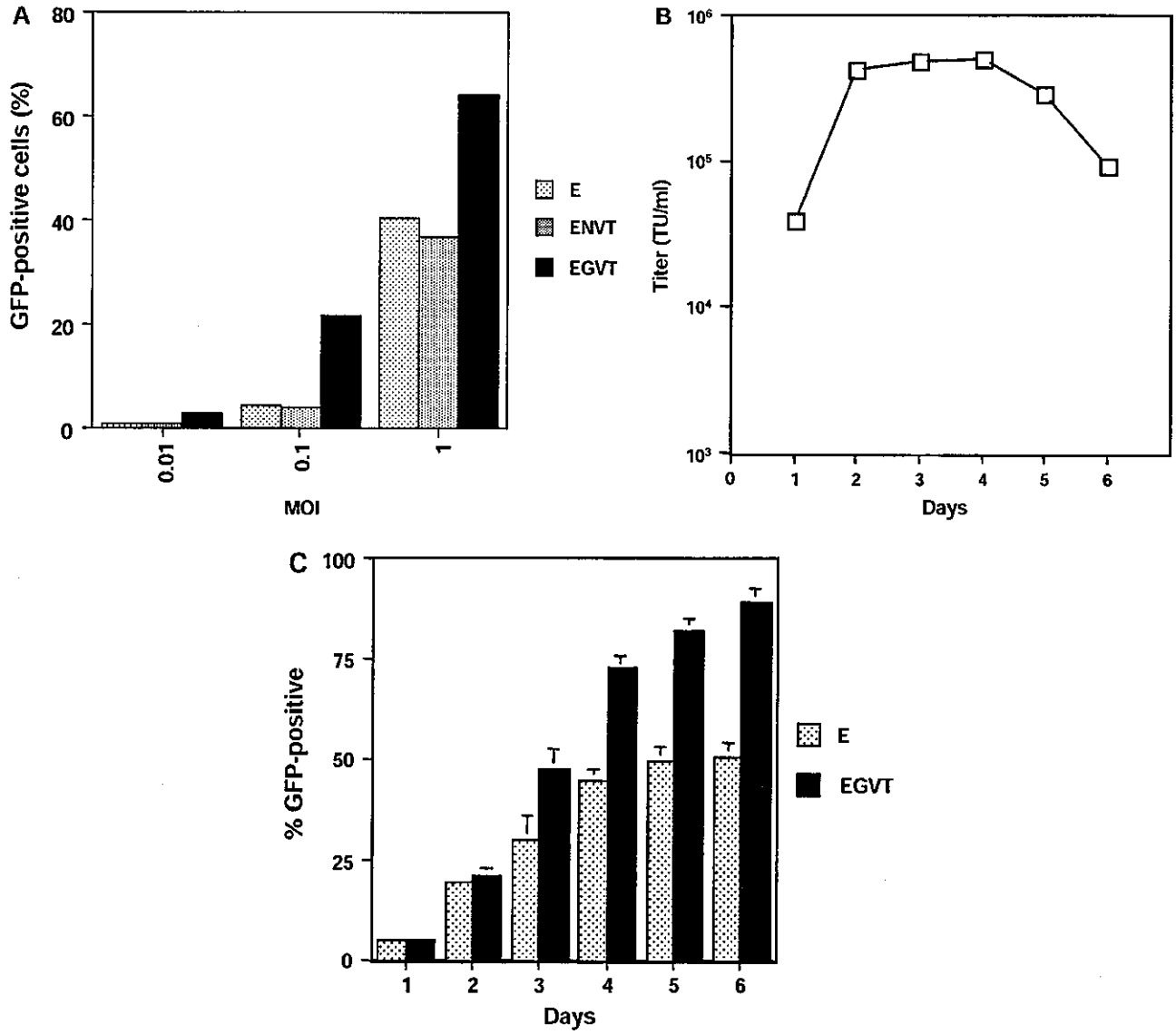

Figure 3. Transduction efficiency of the adeno-retroviral hybrid vector system in 9L cells. (A) Rat 9L glioma cells were infected with the trans-complementing adeno-retroviral vectors at a variety of MOIs (0.01, 0.1, and 1 of each virus) in the presence of 1 μg/ml doxycycline. The hybrid adeno-retroviruses used were as follows: AVC2.GCEGFP alone (E), AVC2.GCEGFP, AVC2null, AxTetVSVG, and AV-rtTA (ENVT), or AVC2.GCEGFP, AxTetGP, AxTetVSVG, and AV-rtTA (EGVT). Cells were harvested for FACS analysis of GFP expression 4 days after transduction. (B) Time course of retroviral production by 9L cells infected with the hybrid vectors. Cells were infected with AVC2.GCEGFP, AxTetGP, AxTetVSVG, and AV-rtTA at an MOI of 3 of each virus in the presence of doxycycline. At different time points, the medium was replaced and the supernatant was titrated for EGFP expression on 293 cells. Data shown represent means from three independent experiments. (C) The percentage of EGFP-positive cells transduced with the hybrid vectors was determined at various time points by FACS. Cells were infected with AVC2.GCEGFP (E) or with AVC2.GCEGFP, AxTetGP, AxTetVSVG, and AV-rtTA (EGVT) at an MOI of 3 of each virus in the presence of doxycycline. Data shown represent means and standard deviations from three independent experiments

Characterization of an adeno-retroviral vector carrying the HSV-*tk* gene

To demonstrate that the retroviral vector cassette within AVC2.GCTK could be used as a retroviral genome template, the retroviral producer cell line FLYA13 was transduced with the adeno-retroviral hybrid vector AVC2.GCTK at an MOI of 10. The retroviral supernatants harvested 48 h post-transduction gave a titer of 1×10^7 TU/ml, which is consistent with titers obtained using this cell line for the conventional production of retrovirus [5].

To examine the generation of the progeny retroviruses in glioma cells using this AVC2.GCTK adeno-retroviral vector system, we transduced rat glioma 9L cells with this vector and the trans-complementing adenovirus carrying the retroviral gag-pol and VSV-G proteins at an MOI of 10 for each, followed by doxycycline treatment. The retroviral titer of supernatants harvested 4 days after transduction, as measured by RNA dot blot analysis, was estimated to be 4×10^5 TU/ml. This experiment was performed several times using different pools of supernatants and produced similar results in all cases.

The HSV-*tk* adeno-retrovirus enhances GCV pro-drug killing of glioma cells

To assess if the killing effect of HSV-*tk* and GCV is enhanced as a result of the use of our adeno-retroviral hybrid vector system, a GCV-sensitivity assay was performed using a mixture of transduced and non-transduced 9L cells at a ratio of 1:19 or 1:9. Three different groups of transduced 9L cells were studied: (1) cells transduced with AVC2.null alone (MOI 40); (2) cells transduced with AVC2.GCTK, AVC2.null, AxTetVSVG, and AV-rtTA (MOI of 10 each); and (3) cells transduced with AVC2.GCTK, AxTetGP, AxTetVSVG, and AV-rtTA) (MOI of 10 each). The cells were analyzed for GCV sensitivity 48 h post-transduction. A dose range of GCV was used (0.01–100 μM). Representative data are shown in Figure 4. In the presence of GCV, infected cells mixed with non-infected cells at a ratio of 5% to 95% that were transduced with all the adeno-retroviral vectors except that AxTetGP, which is required for the generation of retrovirus, had an IC50 value of 46.8 μM (Figure 4A). In contrast, 9L transduced with the progeny-producing combination of adeno-retroviruses had an IC50 value of 1.1 μM. The increase in sensitivity to GCV that the ability to produce progeny conferred to the 9L glioma cells is thus more than one log. Similar results were obtained when infected cells were mixed with non-infected cells at a ratio of 10% to 90% (Figure 4B).

Proviral integration

The generation of an integrated HSV-*tk* provirus by trans-complementation of the adeno-retroviral vectors was verified by analysis of the flanking retroviral LTR sequences. Typical retrovirus reverse transcription and integration resulted in the re-duplication of the 3′ LTR of the retrovirus to form the 5′ LTR (Figure 5A). The 5′ and 3′ LTR sequences of the retroviral vector in the original adeno-retroviral vector differed slightly as the 5′ LTR was derived from MMLV and the 3′ LTR was from MPSV. Re-duplication of the 3′ LTR as the result of retroviral transduction, reverse transcription, and integration should result in the generation of two LTRs with the same sequence. To assess if the expected re-duplication of the 3′ LTR occurred following the transduction of 9L cells with the trans-complementing adenoviruses and the AVC2.GCTK adeno-retroviral vector, we extracted high molecular weight cellular DNA from the cells transduced with AVC2.GCTK, AxTetGP, AxTetVSVG, and AV-rtTA. A PCR product of the expected size was amplified from the DNA sequences within the LTR to a region downstream of 5′ LTR. *Xba* I digestion of the PCR product resulted in the generation of fragments of the expected size, which suggests that the 3′ LTR had been converted into the 5′ LTR following the generation of progeny retrovirus (Figure 5B).

Therapeutic effect of the HSV-*tk* adeno-retroviral vector system *in vivo*

To assess if intratumoral administration of the trans-complementing HSV-*tk* adeno-retroviral vectors leads to the *in situ* production of a retrovirus expressing HSV-*tk* and thus enhanced sensitivity to GCV killing, 9L tumors established in *nu/nu* mice were injected with either AVC2.null alone (n = 20, group 1), AVC2.GCTK alone (n = 20, group 2), AVC2.GCTK, AVC2.null, AxTetVSVG, and AV-rtTA (n = 20, group 3), or AVC2.GCTK, AxTetGP, AxTetVSVG, and AV-rtTA (n = 16, group 4). Subsequently, half the animals in each group (n = 10 or 8 in each group) received intraperitoneal injections of either PBS or GCV. Figure 6 shows the tumor size in *nu/nu* mice after vector administration. Compared with treatment with combinations that are insufficient for retrovirus production, treatment with the ideal combination of vectors significantly inhibited the growth of the established tumors (group 4 vs. group 3 plus GCV, $p < 0.05$ by the

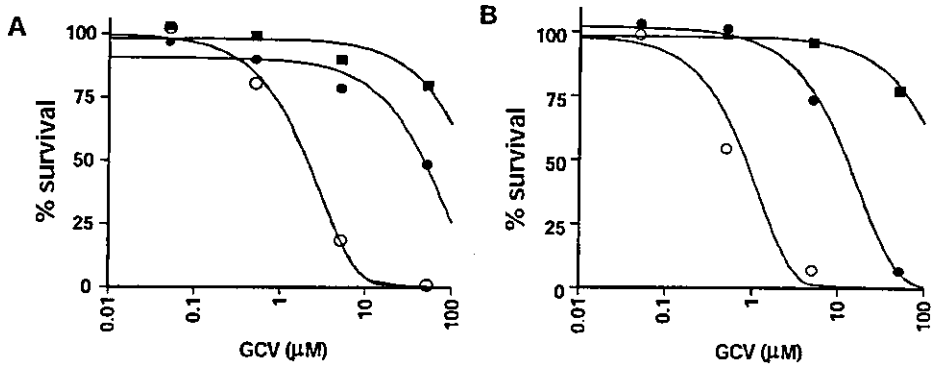

Figure 4. Enhanced killing of rat 9L glioma cells following transduction with adeno-retroviral vectors. GCV-sensitivity assays were performed using mixtures of transduced and non-transduced 9L cells at a ratio of 1:19 (A) or 1:9 (B). Three different groups of transduced cells were used, namely, (1) AVC2.null at an MOI of 40 (■); (2) AVC2.GCTK, AVC2null, AxTetVSVG, and AV-rtTA (MOI of 10 for each) (●); and (3) AVC2.GCTK, AxTetGP, AxTetVSVG, and AV-rtTA (MOI of 10 for each) (○). The transduced 9L cells were harvested 48 h post-transduction and the killing effect of GCV was measured by ^{3}H-thymidine incorporation. The effect on tumor cell proliferation is expressed as a percentage of the thymidine incorporation found in identical cultures that had not been treated with GCV